Naturally small Dirac neutrino mass with intermediate $\mathrm{SU}(2)_L$ multiplet fields

Weijian Wang[a] **and Zhi-Long Han**[b]

[a]*Department of Physics, North China Electric Power University,*
Baoding 071003, China
[b]*School of Physics, Nankai University,*
Tianjin 300071, China

E-mail: wjnwang96@aliyun.com, hanzhilong@mail.nankai.edu.cn

ABSTRACT: If neutrinos are Dirac fermions, certain new physics beyond the standard model should exist to account for the smallness of neutrino mass. With two additional scalars and a heavy intermediate fermion, in this paper, we systematically study the general mechanism that can naturally generate the tiny Dirac neutrino mass at tree and in one-loop level. For tree level models, we focus on natural ones, in which the additional scalars develop small vacuum expectation values without fine-tuning. For one-loop level models, we explore those having dark matter candidates under Z_2^D symmetry. In both cases, we concentrate on $\mathrm{SU}(2)_L$ multiplet scalars no larger than quintuplet, and derive the complete sets of viable models. Phenomenologies, such as lepton flavor violation, leptogenesis, DM and LHC signatures are briefly discussed.

KEYWORDS: Beyond Standard Model, Discrete Symmetries, Neutrino Physics

ARXIV EPRINT: 1611.03240

Contents

1 Introduction

The mechanism responsible for tiny neutrino mass generation remains a puzzle. If the neutrinos are Majorana particles, the attractive scenario is to introduce Weinberg's dimension five operator $\lambda LL\Phi\Phi/\Lambda$ [1], where Λ is the typical high energy scale of underlying new physics. By adding new heavy intermediate states to the Standard Model (SM) particle content, there are three canonical mechanisms to realize above operator at tree level (referred to as type-I, II, III seesaw models [2–9]). The smallness of neutrino mass can also be achieved at low energy scale, either by pushing the mass operator beyond five dimension [10–19] or by attributing the mass term to purely radiative arising at loop-level (sees ref. [20–26] for classic examples). In these models, new physics may arise at TeV scale and thus be detectable at LHC or other planned collider machine [27–33]. In ref. [18], the minimal realizations of the seesaw mechanisms at tree level are listed according to the nature of heavy intermediate $SU(2)_L$ multiplet fermions. In ref. [34], the one-loop neutrino mass model proposed by Ma [22] is generalized to a class of related models with $SU(2)_L$ multiplet fields no larger than adjoint representation.

On the other hand, the experimental evidences establishing whether neutrinos are of Majorana or Dirac type are still missing. If neutrinos are Dirac particles and acquire their masses via direct coupling with SM Higgs boson, the Yukawa coupling constants have to be unnaturally small in comparison with other SM fermions. To solve the problem, some mechanism accounting for the smallness of Dirac neutrino mass have been proposed by

many authors at tree (see ref. [35–42] for earlier works and ref. [43–49] for latest works) and loop level [50–59]. In ref. [57], the generic topographies of diagrams with specific cases are presented.

In this work, we catalogue the related models that generate the tiny Dirac neutrino mass at tree and one-loop level. In section 2, we focus on the minimal tree level realizations of Dirac seesaws with at most two extra scalars $S_{1,2}$ and a heavy intermediated Dirac fermion F, see figure 1. As pointed out in ref. [57], to obtain a naturally small Dirac neutrino mass, another symmetry is required to forbid the $\bar{\nu}_L \nu_R \overline{\phi^0}$ term, where ϕ^0 denotes the SM Higgs field. Then the breaking of this symmetry induces the effective Dirac neutrino mass $m_D \bar{\nu}_L \nu_R$. It naively appears that, by adding appropriate $SU(2)_L$ multiplet field variants to SM, there are infinite ways to realize tree level diagram in figure 1. However, we will see that, as the Majorana case [18], the number of candidate models is significantly reduced if only the models with non-tuning vacuum expectation values (VEVs) are considered.

At one-loop level, a typical diagram was proposed [50, 51, 57], in which the particle content includes two extra scalars and a gauge-singlet fermion being odd under Z_2 symmetry. As a result, the lightest beyond-SM field is stable and may be considered a dark matter (DM) candidate. In section 3, we generalize the approach given in ref. [34]. We list a class of models which generates the Dirac neutrino masses via the one-loop diagram in figure 2 and simultaneously includes a DM candidate. Without loss of generality, we mainly restrict our attention on the models with the $SU(2)_L$ multiplets fields no larger than adjoint while briefly list the models with larger multiplets in appendix. For each model, we investigate its validity and the type of DM candidate which is compatible with direct detection experiments. We consider the phenomenology of the models in section 4. discussing the issues of lepton number violation processes, leptogenesis and collider signals. A conclusion is given in section 5.
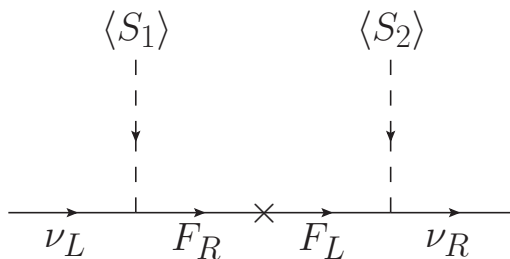
2 Tree level models for Dirac neutrino mass

Pathways to naturally small Dirac neutrino mass have been recently discussed in ref. [57]. By adding an extra Dirac fermion singlet/doublet/triplet or scalar doublet, four tree-level seesaw models are found to realize the Dirac neutrino mass generation. However, the Dirac seesaw mechanism is more general when we move beyond the field content given in ref. [57]. Following the spirit of ref. [18, 19], we firstly discuss the tree-level realization of Dirac seesaw with at most two extra scalars $S_{1,2}$ and a heavy intermediated Dirac fermion F[1] (figure 1). Here, the global lepton number symmetry $U(1)_\ell$ is proposed to forbid the unwanted Majorana mass term $(m_N/2)\overline{\nu_R^C}\nu_R$, meanwhile the discrete Z_3 [55, 58], Z_4 [48, 60, 61] and $\Delta(27)$ [62] symmetry are also optional.

In order to obtain a naturally small Dirac neutrino mass, another symmetry $\mathcal{S}$ is required to forbid the $\bar{\nu}_L \nu_R \overline{\phi^0}$ term. Then the broken of this symmetry $\mathcal{S}$ induces the effective Dirac neutrino mass term $m_D \bar{\nu}_L \nu_R$ [57]. The choice of symmetry $\mathcal{S}$ is model-dependent and here we take the Z_2 symmetry as an example. In table 1, we show two

---

[1]Here, we introduce three generations of heavy fermion F. For simplicity, we will not show the generation indices explicitly in the following discussion.

Figure 1. Dirac neutrino mass at tree level.

Cases	L_L	S_1	F_R	F_L	S_2	ν_R
(A)	$+$	$-$	$-$	$-$	$+$	$-$
(B)	$+$	$+$	$+$	$+$	$-$	$-$

Table 1. Cases of Z_2-charge assignments for relevant fields.

possible cases of Z_2-charge assignment for relevant fields. Under the Z_2 symmetry, ν_R is Z_2-odd while other SM particles are Z_2-even in all cases, which is aiming to forbid the $\bar{\nu}_L \nu_R \overline{\phi^0}$ term. Since F_L carries same Z_2-charge as F_R, $M_F \bar{F}_L F_R$ is invariant under Z_2 as well as SM gauge symmetry. Therefore, M_F could be assumed as large as 1 TeV. The Z_2 symmetry is broken explicitly by terms as $H S_1 S_2$, because of opposite Z_2-charge assignment of S_1 and S_2 for both case (A) and (B) in table 1. Note that if terms as $S_{1,2} H^n (n \leq 3)$ exist, they could explicitly break the Z_2 symmetry as well.

Some generic features are described from the general tree level diagram in figure 1:

- The heavy fermion F is vector-like, which transforms as $F_{L,R} \sim (1, R_F, Y_F)$ under the $\mathrm{SU}(3)_C \times \mathrm{SU}(2)_L \times \mathrm{U}(1)_Y$ gauge symmetry.

- The scalars $S_{1,2}$ transform as $S_{1,2} \sim (1, R_{1,2}, Y_{1,2})$, and they are necessarily distinct from each other, i.e., $R_1 \neq R_2$ or/and $Y_1 \neq Y_2$.

- The new particles F and $S_{1,2}$ must contain a neutral component, which requires:

$$|Y_i| \leq R_i - 1, \quad (i = F, 1, 2).$$ (2.1)

  And Y_i must be an integer to avoid fractionally charged particles as well.

- For isospin allowing to couple F and $S_1(S_2)$ to $L_L(\nu_R)$, following relations should be satisfied:

$$R_L \otimes R_1 \supset R_F \Rightarrow |R_1 - R_F| = 1,$$ (2.2)
$$R_\nu \otimes R_2 \supset R_F \Rightarrow R_2 = R_F,$$ (2.3)

where $R_L = 2$ and $R_\nu = 1$ are the isospin values for SM lepton doublet L_L and neutrino singlet ν_R, respectively.

- The neutrality of hyper charge Y then requires that:

$$-Y_F + Y_L + Y_1 = 0 \;\Rightarrow\; Y_1 = Y_F + 1\,, \tag{2.4}$$

$$-Y_\nu + Y_F + Y_2 = 0 \;\Rightarrow\; Y_2 = -Y_F\,, \tag{2.5}$$

where $Y_L = -1$ and $Y_\nu = 0$ are the hyper charges for SM lepton doublet L_L and neutrino singlet ν_R, respectively.

- Considering the above relations in eq. (2.2)–(2.5) as well as the fact that the SM Higgs H has the quantum numbers as $R_H = 2 = R_L$ and $Y_H = 1$, one can deduce the following relations:

$$(R_H \otimes R_1) \otimes R_2 \supset 1\,, \tag{2.6}$$

$$Y_1 + Y_2 - Y_H = 0\,, \tag{2.7}$$

which indicates that a trilinear term as $\tilde{H}S_1 S_2$ is always allowed in the scalar potential. Here, $\tilde{H} = i\sigma_2 H^*$ is the conjugate of the SM Higgs doublet.

We arrive at the relevant terms to generate small Dirac neutrino masses as shown in figure 1:

$$\mathcal{L} \supset y_1 \overline{F_R} L_L S_1 + y_2 \overline{\nu_R} F_L S_2 + M_F \overline{F_L} F_R + \mu \tilde{H} S_1 S_2 + \text{h.c.} \tag{2.8}$$

Then the generic form of Dirac seesaw mechanism is realized, for which the neutrino mass from tree level contribution is given by

$$m_\nu^{\text{tree}} \simeq y_1 y_2 \frac{\langle S_1 \rangle \langle S_2 \rangle}{M_F}\,. \tag{2.9}$$

For $m_\nu^{\text{tree}} \sim 0.1\,\text{eV}$, one can set $y_1 \sim y_2 \sim 10^{-2}$, $\langle S_1 \rangle \sim \langle S_2 \rangle \sim 10^{-2}\,\text{GeV}$, and $M_F \sim 10^2\,\text{GeV}$. It is an important issue on how S_1 and S_2 develop naturally small VEV comparing to H, which will be discussed in the following. Before proceeding, one notes that the trilinear $\mu \tilde{H} S_1 S_2$ term also contributes to Dirac neutrino mass via the one-loop diagram in figure 2. Actually, if the VEVs of S_1 and S_2 are forbidden by an additional symmetry, e.g., Z_2^D or $\text{U}(1)_D$, only loop diagram can exist and contribute to the neutrino mass generation. In this case, it is possible to include dark matter candidates running in the loop, which is postponed for a more detail discussion in section 3.

For the sake of simplicity, one assumes a degenerate mass spectrum for particles within F, S_1 and S_2, then the one-loop contribution to Dirac neutrino mass is given by

$$m_\nu^{\text{loop}} = C_\nu \frac{\sin 2\theta}{32\pi^2} y_1 y_2 M_F \left[\frac{M_{S_2}^2}{M_{S_2}^2 - M_F^2} \ln\left(\frac{M_{S_2}^2}{M_F^2}\right) - \frac{M_{S_1}^2}{M_{S_1}^2 - M_F^2} \ln\left(\frac{M_{S_1}^2}{M_F^2}\right) \right], \tag{2.10}$$

where θ is the mixing angle between S_1 and S_2. The coefficient C_ν is determined by different particle sets running in the loop and the corresponding Clebsch-Gordan coefficients, thus is model dependent. For example, in model (a) listed in table 3 where $F \sim (1,1,0)$, $S_1 \sim (1,2,1)$ and $S_2 \sim (1,1,0)$, we have $C_\nu = 1$. Depending on relative values between
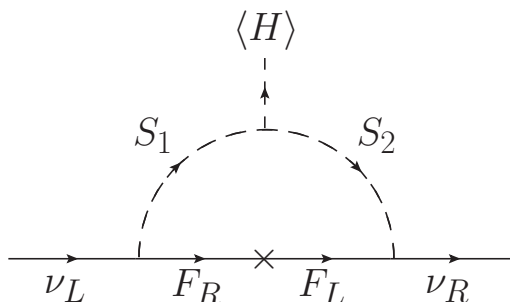
Figure 2. Dirac neutrino mass at one-loop level.

M_F and $M_{S_{1,2}}$, the expression of $m_\nu^{\rm loop}$ in eq. (2.10) can be further simplified. In the heavy fermion limit with $M_F \gg M_{S_{1,2}}$,

$$m_\nu^{\rm loop} \simeq C_\nu \frac{\sin 2\theta}{32\pi^2} \frac{y_1 y_2}{M_F} \left[M_{S_1}^2 \ln\left(\frac{M_{S_1}^2}{M_F^2}\right) - M_{S_2}^2 \ln\left(\frac{M_{S_2}^2}{M_F^2}\right) \right]. \tag{2.11}$$

While in the opposite limit with $M_F \ll M_{S_{1,2}}$,

$$m_\nu^{\rm loop} \simeq C_\nu \frac{\sin 2\theta}{32\pi^2} y_1 y_2 M_F \ln\left(\frac{M_{S_2}^2}{M_{S_1}^2}\right). \tag{2.12}$$

And at last, when $M_F \approx M_{S_{1,2}}$,

$$m_\nu^{\rm loop} \simeq C_\nu \frac{\sin 2\theta}{32\pi^2} \frac{y_1 y_2}{M_F} (M_{S_2}^2 - M_{S_1}^2). \tag{2.13}$$

Considering the case of comparable masses with $M_F \approx M_{S_{1,2}}$ around electroweak scale, we have

$$\frac{m_\nu^{\rm loop}}{m_\nu^{\rm tree}} \sim \frac{\sin 2\theta}{32\pi^2} \frac{M_{S_2}^2 - M_{S_1}^2}{\langle S_1 \rangle \langle S_2 \rangle}. \tag{2.14}$$

Therefore, the tree level contribution might be dominant provided that $\langle S_{1,2} \rangle$ is not too small.

It seems that there could be an infinite number of models satisfying the above generic features. But when considering constraints from perturbative unitarity[2] [63, 64], we will concentrate on $SU(2)_L$ scalar multiplet no larger than quintuplet in this paper. Meanwhile, the number of candidate models could be significantly reduced when we only consider the models with non-tuning VEVs for additional scalars $S_{1,2}$ [18]. Then, as we shall see, the viable models are finite and we would like to specify all of them.

First, we consider the simplest case when one of S_1 and S_2 is the SM Higgs doublet H. Following the conditions in eq. (2.2)–(2.5), one can figure out four simplest models as: $S_1 = H \sim (1,2,1)$, $F \sim (1,2\mp1,0)$, $S_2 \sim (1,2\mp1,0)$ and $S_1 \sim (1,2\mp1,0)$, $F \sim (1,2,-1)$,

---

[2]The $2 \to 2$ tree-level processes of scalar multiplet pair annihilation into electroweak gauge bosons receive large contribution for scalar multiplet with large weak charge. So the upper limits on isospin and hypercharge of a scalar multiplet can be obtained by requiring that the zeroth partial wave amplitude satisfies the unitarity bound.

$S_2 = H \sim (1, 2, 1)$, which exactly correspond to the cases in ref. [57]. At the same time, the trilinear term $\tilde{H}S_1S_2$ becomes $\tilde{H}HS_{1/2}$ and induces a non-zero VEV of $S_{1/2}$

$$\langle S_{1/2}\rangle \simeq \mu \frac{\langle H\rangle^2}{M_{S_{1/2}}^2}\,. \tag{2.15}$$

Notably, the trilinear term $\tilde{H}HS_{1/2}$ could be an explicit Z_2 breaking term as in the cases (A) and (B) shown in table 1. Thus the small $\langle S_{1/2}\rangle$ is acquired in the technically natural limit of $\mu \ll \langle H\rangle$ even for $M_{S_{1/2}}$ around electroweak scale. Then the tree level neutrino mass in eq. (2.9) is expressed as:

$$m_\nu^{\rm tree} \simeq y_1 y_2 \frac{\mu \langle H\rangle^3}{M_F M_{S_{1/2}}^2}\,. \tag{2.16}$$

Typically, we can acquire $m_\nu^{\rm tree} \sim 0.1\,{\rm eV}$ by seting $y_{1,2} \sim 10^{-2}$, $\mu \sim 1\,{\rm MeV}$, and $M_F \sim M_{S_{1/2}} \sim 1\,{\rm TeV}$. Provided $M_{S_{1/2}} \sim M_F = M$, the tiny tree level Dirac neutrino mass is generated from a dimension $d = 6$ effective low-energy operator as $\mathcal{O}_\nu = \mu \overline{\nu_R} L_L H^3 / M^3$.

Notably, a special case, the so-called neutrinophilic two Higgs doublet model (ν2HDM), appears in literature [47, 65–67], where the new scalar doublet $\eta \sim (1, 2, 1)$ transforms the same as SM Higgs doublet under SM gauge group but carries some new charge, i.e., Z_2 or U(1) [68–70]. In this model, the new Yukawa coupling $\overline{\nu_R}\tilde{\eta}^\dagger L_L$ is allowed and the small VEV of η can be obtained by adding a soft Z_2 or U(1) breaking term as $\eta^\dagger H$, leading to naturally small Dirac neutrino masses [57]. In this case, the tiny Dirac neutrino mass is generated from a dimension $d = 4$ effective low-energy operator as $\mathcal{O}_\nu = \mu \overline{\nu_R}\tilde{H}^\dagger L_L / M$.

Now we move beyond the simplest case and explore further generations with both S_1 and S_2 being new particles. After the electroweak symmetry breaking, VEVs of $S_{1,2}$ will usually contribute to the W and Z boson masses. Especially, for those scalars with SU(2)$_L$ representation $R_{1,2} > 2$, their VEVs $\langle S_{1,2}\rangle$ will affect the ρ parameter away from the SM value $\rho = 1$ at tree-level, which then leads to tight bound on $\langle S_{1,2}\rangle \lesssim \mathcal{O}(1)\,{\rm GeV}$ [71]. The trilinear $\tilde{H}S_1S_2$ term alone can not ensure that both $\langle S_{1,2}\rangle$ are naturally small in general case. Therefore, in order to produce non-tuning VEVs for $S_{1,2}$, the scalar potential $V(H, S_1, S_2)$ should contain linear S_1 or/and S_2 terms as $S_{1,2}H^n (n \leq 3)$. With these conditions in mind, we find the S_1 or/and S_2 with the quantum numbers as (see ref. [18] for more details):

$$S_{1,2} \sim (1, 2, \pm1), (1, 3, 0), (1, 3, \pm2), (1, 4, \pm1), (1, 4, \pm3)\,. \tag{2.17}$$

On the other hand, if only S_i obtains a naturally small VEV from the term $S_i H^n (n \leq 3)$, the trilinear $\tilde{H}S_1S_2$ term will induce a naturally suppressed VEV for S_j as:

$$\langle S_j\rangle \simeq \mu \frac{\langle S_i\rangle\langle H\rangle}{M_{S_j}^2}\,, \quad \text{for } i \neq j\,. \tag{2.18}$$

Thus we expect $\langle S_j\rangle \lesssim \langle S_i\rangle$, when $\mu \lesssim \langle H\rangle \lesssim M_{S_j}$.

Based on the above statement, the general strategy for determining a specific Dirac seesaw model is quite straight. First, one determines a scalar S_i with quantum number in

Models	F	S_1	S_2	$[\mathcal{O}_\nu]$	style
(A)	$(1,1,0)$	$H(1,2,1)$	$\phi(1,1,0)$	$d=6$	minimal
(B)	$(1,2,-1)$	$\phi(1,1,0)$	$H(1,2,1)$	$d=6$	minimal
(C)	$(1,2,-1)$	$\Delta(1,3,0)$	$H(1,2,1)$	$d=6$	minimal
(D)	$(1,2,1)$	$\Delta(1,3,2)$	$\eta(1,2,-1)$	$d=(4)6$	(non-)minimal
(E)	$(1,3,0)$	$H(1,2,1)$	$\Delta(1,3,0)$	$d=6$	minimal
(F)	$(1,3,0)$	$\chi(1,4,1)$	$\Delta(1,3,0)$	$d=6,8$	non-minimal
(G)	$(1,3,-2)$	$\eta(1,2,-1)$	$\Delta(1,3,2)$	$d=(4)6$	(non-)minimal
(H)	$(1,3,-2)$	$\chi(1,4,-1)$	$\Delta(1,3,2)$	$d=(6)8$	(non-)minimal
(I)	$(1,3,2)$	$\chi(1,4,3)$	$\Delta(1,3,-2)$	$d=8$	minimal
(J)	$(1,4,1)$	$\Delta(1,3,2)$	$\chi(1,4,-1)$	$d=8$	minimal
(K)	$(1,4,1)$	$\Phi(1,5,2)$	$\chi(1,4,-1)$	$d=10$	minimal
(L)	$(1,4,-1)$	$\Delta(1,3,0)$	$\chi(1,4,1)$	$d=8$	minimal
(M)	$(1,4,-1)$	$\Phi(1,5,0)$	$\chi(1,4,1)$	$d=10$	minimal
(N)	$(1,4,3)$	$\Phi(1,5,4)$	$\chi(1,4,-3)$	$d=10$	minimal
(O)	$(1,4,-3)$	$\Delta(1,3,-2)$	$\chi(1,4,3)$	$d=10$	minimal
(P)	$(1,4,-3)$	$\Phi(1,5,-2)$	$\chi(1,4,3)$	$d=10$	minimal
(Q)	$(1,5,0)$	$\chi(1,4,1)$	$\Phi(1,5,0)$	$d=10$	minimal
(R)	$(1,5,2)$	$\chi(1,4,3)$	$\Phi(1,5,-2)$	$d=10$	minimal
(S)	$(1,5,-2)$	$\chi(1,4,-1)$	$\Phi(1,5,2)$	$d=10$	minimal
(T)	$(1,5,-4)$	$\chi(1,4,-3)$	$\Phi(1,5,4)$	$d=10$	minimal

Table 2. Natural tree level seesaws for Dirac neutrinos. For simplicity, we denote new scalar singlet to quintuplet as ϕ, η, Δ, χ and Φ, respectively.

eq. (2.17), and then the viable sets of quantum numbers for F and S_j can be obtained by eq. (2.2)–(2.5). Following this procedure, we have listed all viable models in table 2. Clearly from table 2, naturally small Dirac neutrino mass arises from even number dimension effective operators as $\mathcal{O}_\nu = \overline{\nu_R} L_L H^{2n+1}/\Lambda^{2n}$ and a higher scalar/fermion representation generally tends to a higher dimension effective operator.

Some comments on specific models are as following. Model (A) and (B) contains a scalar singlet $\phi \sim (1,1,0)$. In our consideration, VEV of ϕ is induced from the Z_2 breaking trilinear term $\mu\tilde{H}H\phi$, thus $\langle\phi\rangle \simeq \mu\langle H\rangle^2/M_\phi^2$ is naturally small when $\mu \ll \langle H\rangle \lesssim M_\phi$. Since the VEV of ϕ does not contribute to the ρ-parameters, it may be typically around electroweak scale and originated from the spontaneous breaking of scalar potential [48, 72–74]. In this way, one needs the intermediate fermion F with $\mathcal{O}(10^{10})\,$GeV mass scale to generate proper neutrino masses, just as the canonical type-I seesaw model.

Model (D) and (G) employ a scalar doublet $\eta \sim (1,2,-1)$. Provided η is Z_2-odd as ν_R (as case (B)), the Yukawa coupling $\overline{\nu_R}\eta^\dagger L_L$ is allowed. After η develops a VEV from the soft term $\tilde{\eta}^\dagger H$, the $\overline{\nu_R}\eta^\dagger L_L$ term induces a Dirac mass term corresponding to dimension $d=4$ effective operator as $\mathcal{O}_\nu = \overline{\nu_R}\tilde{H}^\dagger L_L$. Meanwhile, the heavy intermediate fermion F

together with η and another scalar triplet $\Delta\,(1,3,2)$ generate Dirac neutrino mass from $d=6$ effective operator as $\mathcal{O}_\nu = \overline{\nu_R}L_L H^3/\Lambda^2$. Thus, light Dirac neutrino mass have two contributions, which can be written as

$$m_\nu^{\text{tree}} \simeq y_{1/2}\langle\eta\rangle + y_1 y_2 \frac{\langle\eta\rangle\langle\Delta\rangle}{M_F}\,. \tag{2.19}$$

Since $\langle\Delta\rangle \ll M_F$, the Dirac neutrino mass is dominant by the first term in eq. (2.19). Hence, model (D) and (G) are non-minimal, and can be regarded as just a more complicated extension of the ν2HDM with new contributions to Dirac neutrino mass subdominant.

In contrast, if η is Z_2-even as case (A) shown in table 1, we might be able to treat η as the charge-conjugate field of H, i.e., $\eta = \tilde{H}$. In this case, the Yukawa coupling $\overline{\nu_R}\eta^\dagger L_L = \overline{\nu_R}\tilde{H}^\dagger L_L$ is forbidden, so the light Dirac neutrino mass can only be induced by the heavy intermediate fermion F as

$$m_\nu^{\text{tree}} \simeq y_1 y_2 \frac{\langle H\rangle\langle\Delta\rangle}{M_F}\,. \tag{2.20}$$

Then in addition to the four obvious minimal models — model (A), (B), (C) and (E), we get two more minimal models — model (D) and (G) with $d=6$ effective operators as well. When counting on the heavy intermediate fermion, one more representation $F \sim (1,3,-2)$ is employed in model (G), while we can regard $F \sim (1,2,1)$ in model (D) as the charge-conjugate of $F \sim (1,2,-1)$ in model (B) and (C).

For the scalar triplet $\Delta \sim (1,3,\pm2)$ which is involved in model (D), (G), (H), (I) and (J), the $L_L L_L \Delta$ term is forbidden by the unbroken $U(1)_\ell$ lepton symmetry in case of Dirac neutrino. Since for tree level models in this work, we can only assign lepton number $L=1$ or $L=0$ to new fermion F and scalars $S_{1,2}$ (including Δ), respectively.

Comparing with model (E) and (F), it is obvious that model (F) is essentially model (E) with an additional scalar quadruplet $\chi \sim (1,4,1)$. As a result, model (F) is non-minimal, and neutrino mass is generated by two distinct tree level diagrams. And provided $\eta = \tilde{H}$ in model (G), then model (H) is clearly also non-minimal. Under such circumstances, the light neutrino mass for model (F) and (H) is given by:

$$m_\nu^{\text{tree}} \simeq y_1^H y_2 \frac{\langle H\rangle\langle\Delta\rangle}{M_F} + y_1^\chi y_2 \frac{\langle\chi\rangle\langle\Delta\rangle}{M_F}\,, \tag{2.21}$$

which correspond to effective operators of dimension $d=6$ and $d=8$, respectively.

Now let's look at a specific model, i.e., model (K) in table 2, to show how to construct a complete model. First, we choose $S_2 \sim (1,4,-1)$ in eq. (2.17). Then, the quantum number of $F \sim (1,4,1)$ can be obtained from constraints in eq. (2.3), (2.5) by the Yukawa coupling $\overline{\nu_R}F_L S_2$. At last, inspection of constraints in eq. (2.2), (2.4) by the other Yukawa coupling $\overline{F_R}L_L S_1$ reveals that either $S_1 \sim (1,3,2)$ or $S_1 \sim (1,5,2)$ corresponding to model (J) and (K), respectively.

In figure 3, we depict the tree level Dirac seesaw of model (K). The scalar quadruplet $S_2 \sim (1,4,1)$ acquires a naturally small VEV from the quartic term $\lambda S_2^\dagger H H^\dagger \tilde{H}$ as:

$$\langle S_2\rangle \simeq \lambda \frac{\langle H\rangle^3}{M_{S_2}^2}\,. \tag{2.22}$$

– 8 –
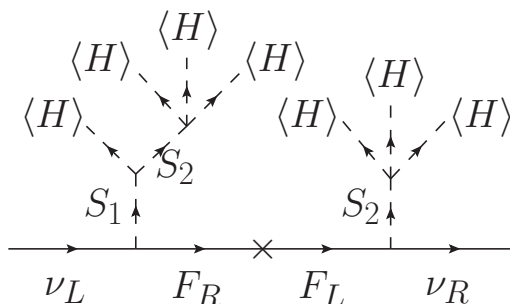
Figure 3. Tree level Dirac seesaw of model (K) in table 2.

For the scalar quintuplet $S_1 \sim (1, 5, 2)$, the trilinear $\tilde{H}S_1S_2$ term ensures S_1 also develops a naturally small VEV as shown in eq. (2.18):

$$\langle S_1 \rangle \simeq \mu \frac{\langle S_2 \rangle \langle H \rangle}{M_{S_1}^2} \simeq \lambda \frac{\mu \langle H \rangle^4}{M_{S_1}^2 M_{S_2}^2} \,. \tag{2.23}$$

As a consequence, the tree level Dirac neutrino mass in model K is:

$$m_\nu^{\text{tree}} \simeq y_1 y_2 \frac{\langle S_1 \rangle \langle S_2 \rangle}{M_F} \simeq y_1 y_2 \frac{\lambda \mu}{M_F} \frac{\langle H \rangle^7}{M_{S_1}^2 M_{S_2}^4} \,. \tag{2.24}$$

Supposing $\mu \sim M_{S_{1,2}} \sim M_F = M$, then we have $m_\nu^{\text{tree}} \propto \langle H \rangle^7 / M^6$, which indicates that the tiny Dirac neutrino mass is induced by a dimension $d = 10$ effective operator as $\mathcal{O}_\nu = \overline{\nu_R} L_L H^7 / M^6$.

3 One-loop models for Dirac neutrino mass

Now, we move forward to the purely radiative generation of Dirac neutrino mass. There were variant of models proposed in this direction. At one-loop level, the simplest model discussed in ref. [75] is based on soft-broken Z_2 symmetry, where two new charged scalar singlets are employed. However, no DM candidate can be incorporated in this model. Another appealing way is introducing an additional symmetry, e.g., a dark Z_2 symmetry (Z_2^D), under which $S_{1,2}$ and F carry Z_2^D-odd charge while all SM fields transform trivially. In this way, the VEVs of $S_{1,2}$ is forbidden and neutrino mass can only be generated via the one-loop diagram shown in figure 2. Due to the Z_2^D odd protection, the lightest neutral component within the inert fields $S_{1,2}$ or F is stable, and thus becomes a DM candidate. In this paper, we restrict our attention on the models involving neutral components and analyze their validity as a DM. We focus on models with representations no larger than the adjoint representation, and then briefly discuss larger multiplets with quadruplet and/or quintuplet of $SU(2)_L$.

From figure 2, it reveals that, with slightly modification of statements around eq. (2.1), they are still applicable for one-loop case. The difference comes from the fact that in loop models the neutral field does not have to propagate inside the loop, hence we only require that at least one of the new fields $S_{1,2}$ and F has a neutral content. The other constraints,

Models	F	S_1	S_2	Z_2^D DM
(a)	$(1, 1, 0)$	$\eta(1, 2, 1)$	$\phi(1, 1, 0)$	Inert singlet or doublet
(b)	$(1, 1, -2)$	$\eta(1, 2, -1)$	$\phi(1, 1, 2)$	Inert doublet
(c)	$(1, 2, -1)$	$\phi(1, 1, 0)$	$\eta(1, 2, 1)$	Inert singlet or doublet
(d)	$(1, 2, -1)$	$\Delta(1, 3, 0)$	$\eta(1, 2, 1)$	Inert doublet or triplet
(e)	$(1, 2, 1)$	$\phi(1, 1, 2)$	$\eta(1, 2, -1)$	Inert doublet
(f)	$(1, 2, 1)$	$\Delta(1, 3, 2)$	$\eta(1, 2, -1)$	Inert doublet or triplet
(g)	$(1, 2, -3)$	$\Delta(1, 3, -2)$	$\eta(1, 2, 3)$	Excluded
(h)	$(1, 3, 0)$	$\eta(1, 2, 1)$	$\Delta(1, 3, 0)$	Inert doublet or triplet
(i)	$(1, 3, -2)$	$\eta(1, 2, -1)$	$\Delta(1, 3, 2)$	Inert doublet or triplet
(j)	$(1, 3, 2)$	$\eta(1, 2, 3)$	$\Delta(1, 3, -2)$	Excluded

Table 3. Radiative neutrino mass for Dirac neutrinos with DM candidate.

i.e., eq. (2.2)–(2.7), are directly coming or indirectly derived from the relevant Yukawa coupling, so they are still capable for loop models.

With the comments given above, a systematic analysis is made to exhaust the models that generate Dirac neutrino mass via figure 2. In table 3, we list all possible distinct models with representations no larger than the adjoint representation. There are totally ten viable models, and the simplest three of them, i.e., model (a), (c) and (e), are already mentioned in ref. [57]. For models with quadruplet and/or quintuplet, we depict them in table 4.

The generic one-loop Dirac neutrino mass matrix has already been given in eq. (2.10). The trilinear term $\mu \tilde{H} S_1 S_2$ still induces the mixing between inert scalars S_1 and S_2, meanwhile the newly employed Z_2^D symmetry forbids the mixing between $S_{1,2}$ and SM Higgs doublet H. To acquire $m_\nu^{\text{loop}} \sim 0.1\,\text{eV}$, we can set $y_1 \sim y_2 \sim \theta \sim 10^{-3}$ with all inert particles around $\mathcal{O}(\text{TeV})$.

A detailed study on the DM phenomenology for all models presented in table 3 and 4 is beyond the scope of this paper. First, we briefly discuss viable DM candidate in specific models in this section. Then in the next section, we choose model (a) as our benchmark model for a more detail study.

First, we turn our intention into fermion DM candidate. In model (a), an inert fermion singlet $F \sim (1, 1, 0)$ is introduced. Possible annihilation channels are: 1), $F\bar{F} \to \ell^+\ell-, \nu\bar{\nu}$ mediated by η via the Yukawa coupling y_1; 2), $F\bar{F} \to \nu\bar{\nu}$ mediated by ϕ via the Yukawa coupling y_2; 3), coannihilation with $\eta(\phi)$, when $M_{\eta(\phi)}$ is close to M_F. For all these channels, not too small Yukawa couplings y_1 and/or y_2 of $\mathcal{O}(0.1)$ are required to generate the correct relic density for electroweak scale F [76, 77]. On the other hand, for η involved channels, the Yukawa coupling y_1 receives tight constraints from lepton flavor violating processes [77]. Therefore, we expect that the Yukawa couplings satisfy the relation $y_1 \ll y_2$, which further indicates that the ϕ mediated process is dominant provided $M_\phi \approx M_\eta$.

Another notable model with viable fermion DM is model (h), where an inert fermion triplet $F \sim (1, 3, 0)$ is introduced. The neutral component F^0 can serve as a DM candidate.

Due to its electroweak couplings to gauge bosons, the relic density of F^0 is dominantly determined by the annihilation and co-annihilation of itself and $F^\pm$, which requires that M_{F^0} is around 2.6 TeV [78–80]. In this case, $S_1 \sim (1, 2, 1)$ and $S_2 \sim (1, 3, 0)$ should be heavier than 2.6 TeV, thus hardly being tested at LHC.

Fermion DM in other models with no larger than adjoint representation are excluded. Clearly, for model (b) and (g), $F \sim (1, 1, -2)$ and $F \sim (1, 2, -3)$ do not have neutral component, thus these two models do not have fermion DM candidate. On the other hand, model (c), (d), (e), (f) employ $F \sim (1, 2, \pm 1)$ and model (i), (j) employ $F \sim (1, 3, \pm 2)$, which contain neutral fermions. But all the neutral fermions in these model have non-zero hypercharge, which will lead to detectable DM-nucleon scattering cross section via Z-boson exchange. So they have already been excluded by direct detection experiments, such as, LUX [81–83] and PandaX-II [84].

Then we move onto scalar dark matter. Considering the constraints from LFV and tiny neutrino masses, it is better to set the Yukawa coupling $y_1 \sim y_2 \lesssim 10^{-2}$. In this way, the contribution of heavy fermion F to scalar DM variables is negligible. Both model (a) and (c) introduce an inert scalar singlet $\phi \sim (1, 1, 0)$ [85, 86] and an inert scalar doublet $\eta \sim (1, 2, 1)$ [87–89]. In principle, either of ϕ and η can solely paly the role of dark matter candidate under the Z_2^D symmetry. In these two models, the trilinear term $\mu \phi \eta^\dagger H / \sqrt{2}$ will induce the mixing between ϕ and η_R^0, and the allowed parameter space thus are expected enlarged. Detail phenomenological aspects for inert singlet-doublet scalar dark matter can be found in ref. [90, 91]. From the result of ref. [90, 91], we know that the mixing angle θ between ϕ and η_R^0 must be small enough to avoid too large DM-nucleon scattering cross section if DM is dominant by ϕ component. Notably, there exists a value of $\sin\theta$ for which the correct relic density is maintained only via the four-point gauge interactions when $M_\phi > M_W$. Around this point, the spin-independent detection cross section drops dramatically, since the only tree level contribution from the Higgs boson vanishes. Meanwhile, for $M_\phi < M_W$, the relic density is determined by the Higgs portal. And current direct detection experiments requires that $M_\phi \approx M_h/2$ should be satisfied for light DM [92, 93]. On the other hand if the dark matter is dominant by η component, either η_R^0 or η_I^0, then a mass splitting $\Delta M = |M_{\eta_R^0} - M_{\eta_I^0}| > 100$ keV between η_R^0 and η_I^0 is required to escape the direct detection bound. In these two models, the required mass splitting can be obtained by choosing curtain values of μ in the trilinear term $\mu \phi \eta^\dagger H$ and κ in the quartic term $\kappa(\eta^\dagger H)^2$ [50].

For model (b) and (e), the only DM candidate comes from the inert scalar doublet $\eta \sim (1, 2, -1)$ [87–89], since the other inert scalar $\phi \sim (1, 1, 2)$ is a charged scalar singlet. It is noted that in both models, the neutral components η_R^0 or η_I^0 does not contribute to radiative neutrino mass. Considering the fact that small mixing angle θ between $\phi^\pm$ and $\eta^\pm$ are favored by neutrino mass, the DM phenomenology of η will be quite similar as a standard inert doublet model. Under constraints from relic density, direct detection and indirect detection, there are two mass region allowed for $M_{\eta_R^0/\eta_I^0}$: one is the low mass region with $50 \, \text{GeV} \lesssim M_{\eta_R^0/\eta_I^0} \lesssim 70 \, \text{GeV}$, and the other is the high mass region with $500 \, \text{GeV} \lesssim M_{\eta_R^0/\eta_I^0}$ [87–89]. For the light mass region, pair and associated production processes as $\eta^+ \eta^-$ and $\eta^\pm \eta_R^0/\eta_I^0$ will lead to multi-lepton plus missing transverse energy

$\not{E}_T$ signatures at LHC, which has been extensively studied in ref. [94–98]. While for the high mass region, although hard to be test at LHC, most parameter space of this region is in the reach of CTA experiment [99, 100].

For model (d) and (h), they employ an inert doublet $\eta \sim (1, 2, 1)$ and a real inert scalar triplet $\Delta \sim (1, 3, 0)$ [101–104]. Alternatively, the DM candidate could be either η_R^0/η_I^0 in the inert doublet η or Δ^0 in the inert triplet Δ [105]. If the mass of inert triplet Δ is much heavier than the inert doublet η, we again arrive at the well studied inert doublet model [87–89] as just discussed above. Here, we consider the opposite case where Δ^0 is lighter than the inert doublet η_R^0/η_I^0, and serve as the DM candidate. Determined by the DM relic density, M_{Δ^0} is found to be around 2.5 TeV if (co-)annihilation is via pure gauge coupling, meanwhile the scalar interactions could push M_{Δ^0} up to about 20 TeV due to the Sommerfeld effect [101, 102]. Since Δ^0 does not interact with Z-boson, the DM-nucleon scattering process through the exchange of SM Higgs h at tree level and gauge bosons at one-loop level. And the spin-independent DM-nucleon scattering cross section at one-loop level is calculated as [105]

$$\sigma_{\rm SI} = \frac{g_2^8}{256\pi^3} \frac{f_N^2 m_N^4}{M_W^2} \left[\frac{R_\Delta^2 - 1}{8} \left(\frac{1}{M_W^2} + \frac{1}{M_h^2} \right) - \frac{16\pi}{g_2^4} \frac{\lambda_{h\Delta^0}}{M_h^2} \frac{M_W}{M_{\Delta^0}} \right]^2 \tag{3.1}$$

Here, g_2 is the $SU(2)_L$ gauge coupling, $f_N = 0.3$ is the nucleon matrix element, $m_N = 939$ MeV is the average nucleon mass, $R_\Delta = 3$ is the dimension of inert triplet Δ, and $\lambda_{h\Delta^0}$ is the coupling between the DM Δ^0 and SM Higgs h. For vanishing DM-Higgs coupling $\lambda_{h\Delta^0} = 0$, the spin-independent cross section $\sigma_{\rm SI}$ is 9×10^{-10} pb, which is lower than current LUX bound [81–83]. Remarkably, for certain DM-Higgs coupling, i.e.,

$$\lambda_{h\Delta^0} = \frac{R_\Delta^2 - 1}{8} \frac{g_2^4 M_{\Delta^0}}{16\pi M_W} \left(1 + \frac{M_h^2}{M_W^2} \right) \approx 0.4 \tag{3.2}$$

the spin independent cross section could be suppressed heavily [105], therefore Δ^0 can easily escape direct detection even in the future.

In model (f) and (i), an inert scalar doublet $\eta \sim (1, 2, 1)$ and a complex inert scalar triplet $\Delta \sim (1, 3, 2)$ are added [106]. Naively, we expect that the DM candidate is η_R^0 or η_I^0 in these two models, since Δ_R^0 or Δ_I^0 cannot play the role of DM candidate solely if η does not exist [104]. However, in these two models, a mass splitting $\Delta M = |M_{\Delta_R^0} - M_{\Delta_I^0}|$ between Δ_R^0 and Δ_I^0 exists due to the mixing between η and Δ [107]. Specifically speaking, the quartic term $\kappa(\eta^\dagger H)^2$ will induce the mass splitting between η_R^0 and η_I^0. Then the trilinear term $\mu H^T i\sigma_2 \Delta^\dagger \eta$ will induce the mixing between Δ_R^0 and η_R^0 for the CP-even scalars, and mixing between Δ_I^0 and η_I^0 for the CP-odd scalars, resulting a mass splitting between Δ_R^0 and Δ_I^0. For instance, with $M_{\eta_R^0} = 5$ TeV, $M_{\eta_I^0}^2 = M_{\eta_R^0}^2 - 2\kappa v^2$, $\kappa = 0.5$, $\mu = 1$ TeV, and $M_\Delta = 2.8$ TeV, the mass splitting $\Delta M = |M_{\Delta_R^0} - M_{\Delta_I^0}| \approx 1$ MeV. Therefore this mass splitting ΔM is larger than the DM kinetic energy $\mathcal{O}(100)$ keV, the tree level DM-nucleon scattering via Z-boson is expected kinematically forbidden [34]. In this way, Δ_I^0 (or Δ_R^0 when $\kappa < 0$) can escape the direct detection bound, thus becomes a viable DM candidate. And $M_{\Delta_R^0/\Delta_I^0} \sim 2.8$ TeV is preferred to acquire the correct DM relic density [104].

In model (g) and (j), the only scalar DM candidate is $\Delta \sim (1, 3, -2)$, since the other scalar $\eta \sim (1, 2, 3)$ does not have neutral component. But the scalar triplet Δ has already excluded by the direct detection experiments [104]. Therefore, these two models could not provide viable DM candidate.

Note that the discrete Z_2^D symmetry could be an accidental symmetry of a broken $U(1)_D$ symmetry [108, 109]. Usually, a SM scalar singlet σ is introduced to break $U(1)_D \to Z_2^D$ spontaneously. Under this extended $U(1)_D$ symmetry, the inert fermion F as well as inert scalars $S_{1,2}$ carry certain $U(1)_D$ charges. While all other ingredients could be the same as the Z_2^D case, the quartic term $\kappa(\eta^\dagger H)^2$ for $\eta \sim (1, 2, 1)$ or $\kappa(\eta^T H)^2$ for $\eta \sim (1, 2, -1)$ is forbidden by the $U(1)_D$ symmetry. The absent of this quartic term will lead to degenerate masses of η_R^0 and η_I^0 in model (b) and (e), therefore they will be excluded by direct detection in the case of $U(1)_D$ symmetry. Similar for model (f) and (i), η_R^0 and η_I^0 are degenerate, thus Δ_R^0 and Δ_I^0 are also degenerate. In this way, model (f) and (i) are also excluded. Meanwhile for model (a), (c) or (d), (h), mixing between $\phi \sim (1, 1, 0)/\Delta \sim (1, 3, 0)$ and doublet η can also lead to a mass splitting between η_R^0 and η_I^0. And η_R^0 is the DM candidate when ϕ/Δ is heavier than η.

Last but not least, we give some comments on models with quadruplets or quintuplets in table 4. Obviously, model (m), (n), (q), (r), (s), (v), (w) and (s) have already excluded by direct detection, since the neutral components in these models have non-zero hypercharge and no mass splitting between the real and imaginary part of the neutral fields could be induced. Model (k) and (t) are the only two models with viable fermion DM and quadruplets or quintuplets. For scalar DM, it could be inert triplet or quintuplet with $Y = 0$ as in model (k), (o) and (t). Note that the quartic term $\kappa(\chi^\dagger H)^2$ for $\chi \sim (1, 4, 1)$ or $\kappa(\chi^T H)^2$ for $\chi \sim (1, 4, -1)$ is allowed by the Z_2^D symmetry. Analogy to the inert doublet, this quartic will split the neutral components χ_R^0 and χ_I^0, which makes χ_R^0 or χ_I^0 a viable DM candidate. A mass splitting between real and imaginary part of the neutral fields in triplet/quintuplet, i.e., model (l), (p) and (u), is also possible due to the mixing between triplet/quintuplet and quadruplet. In this way, the corresponding $Y \neq 0$ triplet/quintuplet can avoid the tight direct detection bounds as well in the present of $\chi \sim (1, 4, \pm 1)$.

4 Phenomenology

The natural Dirac seesaw models introduce two additional scalars and a heavy intermediate fermion, which would lead to rich phenomenology. In this section we choose model (B) for tree level models and model (a) for one-loop level models as our benchmark mark models to illustrate the relative phenomenon. We briefly highlight some important aspects, although a detailed research on phenomenology of other specific models is quite necessary.

4.1 Flavor constraints

The existence of Yukawa coupling $y_1 \overline{F_R} L_L S_1$ will induce lepton flavor violation (LFV) processes. Here, we take the current most stringent bound $\mathrm{BR}(\mu \to e\gamma) < 4.2 \times 10^{-13}$ [110, 111] and future limit $\mathrm{BR}(\mu \to e\gamma) < 6 \times 10^{-14}$ [112] to illustrate, and more discussion on
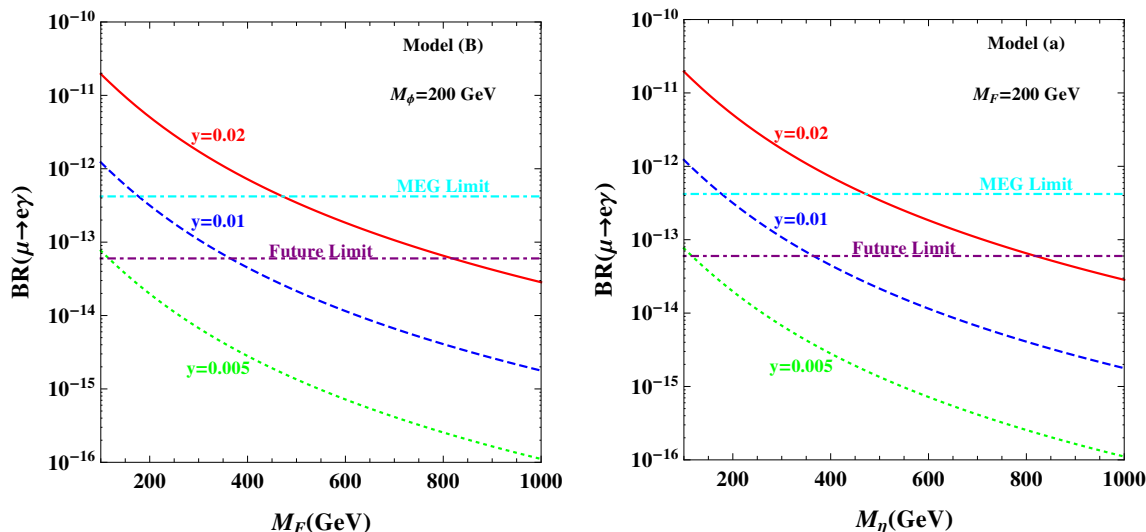
Figure 4. BR($\mu \to e\gamma$) as a function of mass of heavy intermediate particle for tree level model (B) and one-loop level model (a). Here, we assume an universal Yukawa coupling $|y_1^{ij}| = y$ and degenerate masses for the three generation of heavy fermion F for simplicity. We have $S_1 = \phi$ in model (B) and $S_1 = \eta$ in model (a), respectively.

other LFV processes can be found in refs. [113–124]. The general analytical expression for BR($\mu \to e\gamma$) is given by

$$\mathrm{BR}(\mu \to e\gamma) = \frac{3\alpha}{64\pi G_F^2} \left| \sum_{i=1}^{3} \frac{y_1^{ie*} y_1^{i\mu}}{M_{S_1}^2} \left[Q_{F_i} F_1\left(\frac{M_{F_i}^2}{M_{S_1}^2}\right) + Q_{S_1} F_2\left(\frac{M_{F_i}^2}{M_{S_1}^2}\right) \right] \right|^2, \qquad (4.1)$$

where the loop functions $F_i(x)$ are [125]

$$F_1(x) = \frac{2 + 3x - 6x^2 + x^3 + 6x \ln x}{6(1-x)^4}, \qquad (4.2)$$

$$F_2(x) = \frac{1 - 6x + 3x^2 + 2x^3 - 6x^2 \ln x}{6(1-x)^4}. \qquad (4.3)$$

Here, Q_{F_i} and Q_{S_1} denote the electric charge of charged components in F_i and S_1, respectively. More specifically, we have $Q_{F_i} = 1$, $Q_{S_1} = 0$ in model (B) and $Q_{F_i} = 0$, $Q_{S_1} = 1$ in model (a). In figure 4, we depict the predicted value of BR($\mu \to e\gamma$) as a function of charged particle mass in this two models with an universal Yukawa coupling $|y_1^{ij}| = y$ and degenerate masses for the three generation of heavy fermion F. Constraints on the Yukawa coupling for this two models are similar. And for both tree-level model (B) and purely radiative model (a), the tight constraints from LFV usually requires that the corresponding Yukawa coupling $|y_1| \lesssim 0.01$ with F and S_1 around electroweak scale [119–123].

For tree level models, the tight upper bound on branching ratios of LFV could be transformed into a lower bound on $\langle S_1 \rangle$ [125]. From the expression of neutrino mass in eq. (2.9), it is estimated that $y_1 \simeq m_\nu^{1/2} M_F^{1/2}/\langle S_1 \rangle$ by assuming $y_1 \simeq y_2$ and $\langle S_1 \rangle \simeq \langle S_2 \rangle$.

Plugging this estimation into eq. (4.1), one easily derives

$$M_{S_1}\langle S_1 \rangle \gtrsim \left(\frac{3\alpha m_\nu^2 M_F^2}{64\pi G_F^2 \text{BR}(\mu \to e\gamma)} \left| \sum_{i=1}^3 F_1\left(\frac{M_{F_i}^2}{M_{S_1}^2} \right) \right|^2 \right)^{1/4}, \tag{4.4}$$

$$\approx \left[\frac{1 \times 10^{-13}}{\text{BR}(\mu \to e\gamma)} \left(\frac{M_F}{100\,\text{GeV}} \right)^2 \right]^{1/4} \times 600\,\text{GeV} \cdot \text{MeV},$$

where we have assume $m_\nu \sim 0.1\,\text{eV}$ and $\sum F_1(x) \sim 0.1$ in the numerical estimation. For electroweak scale intermediate fermion $M_F \sim 200\,\text{GeV}$, current limits on $\text{BR}(\mu \to e\gamma)$ requires that $M_{S_1}\langle S_1 \rangle \gtrsim 600\,\text{GeV} \cdot \text{MeV}$. Thus, the VEVs of scalars $S_{1,2}$ are expected to be larger than $\mathcal{O}(\text{MeV})$ when the mass of $S_{1,2}$ is around electroweak scale as well.

The contribution to the anomalous magnetic moment of μ can be obtained as a by-product of the above calculation of LFV

$$\Delta a_\mu = \sum_i^3 \frac{|y_1^{i\mu}|^2}{16\pi^2} \frac{M_\mu^2}{M_{S_1}^2} \left[Q_{F_i} F_1\left(\frac{M_{F_i}^2}{M_{S_1}^2} \right) + Q_{S_1} F_2\left(\frac{M_{F_i}^2}{M_{S_1}^2} \right) \right]. \tag{4.5}$$

Under constraints from LFV, the predicted value of Δa_μ is 4×10^{-14} for an universal Yukawa coupling $y_1 \sim 0.01$ and both F and S_1 around electroweak scale, which is clearly too small to interpret the observed discrepancy $\Delta a_\mu = (2.39 \pm 0.79) \times 10^{-9}$ [126].

Another tight constraint comes from electric dipole moments (EDM) of electron, which requires $|d_e| < 8.7 \times 10^{-29}\,e\text{-cm}$ [127]. In all the current Dirac neutrino models, the only new interactions for lepton doublet L_L is the Yukawa coupling $y_1 \overline{F_R} L_L S_1$, which can not give large contributions to EDM at one-loop level [128, 129]. Actually, the contribution of above Yukawa coupling $y_1 \overline{F_R} L_L S_1$ to electron EDM first appears at two-loop level (see figure 4 of ref. [56]). Considering constraints from LFV, a naive estimation for the order of magnitude gives [56]

$$d_e \sim \frac{M_e \,\text{Im}(y_1^2 \lambda)}{(16\pi^2)^2 M_{S_1}^2} \sim 10^{-31}\,e\text{-cm}, \tag{4.6}$$

with $M_{S_1} \sim 200\,\text{GeV}$, $y_1 \sim 0.01$, and $\text{Im}(\lambda) \sim 0.1$. Here, λ is the coefficient of the quartic coupling $S_1^\dagger S_1 H^\dagger H$. Therefore, the contribution of the new Yukawa coupling $y_1 \overline{F_R} L_L S_1$ to electron EDM is about two to three orders of magnitude lower than current limit with the above parameters.

4.2 Leptogenesis

Within Majorana seesaw models, the observed baryon asymmetry can be explained via conventional leptogenesis [130, 131], where the lepton number violation plays an essential role. Obviously, no lepton asymmetry is generated in Dirac seesaw models because the lepton number is conserved. However, the leptogenesis can still be accomplished in Dirac neutrino models [132], due to the fact that the sphaleron processes do not have direct effect on right-handed fields. Therefore, if an equal but opposite amount of lepton asymmetry in the left- and right-handed sectors is created, the lepton asymmetry in the left-handed sector can be converted into a net baryon asymmetry via sphaleron processes, as long as
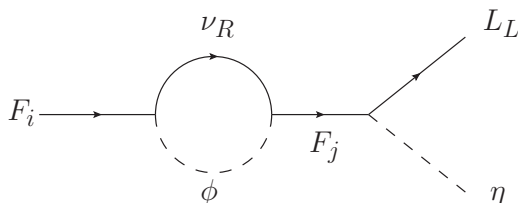
Figure 5. Heavy Dirac fermions F_i decay into left-handed leptons at one-loop level.

the effective Dirac Yukawa couplings are small enough to prevent the lepton asymmetry from equilibration before the electroweak phase transition. Detailed studies on Dirac leptogenesis can be found in ref. [133–140]. For the the models we discussed, the required lepton asymmetry in left- and right-handed sectors arises from the decays of the heavy intermediate fermion F into $L_L S_1$ and $\nu_R S_2$.

For the tree-level model (B), it is possible to generate the baryon asymmetry via resonant leptogenesis with nearly degenerate F_i around TeV-scale [141, 142]. For simplicity, we consider the canonical thermal leptogenesis in the one-loop model (a), where very heavy F_i is needed. The heavy Dirac fermion F_i has two decay modes: $F_i \to L_L \eta$ and $F_i \to \nu_R \phi$, and the corresponding decay widths at tree level are

$$\Gamma(F_i \to L_L \eta) = \Gamma(F_i^C \to L_L^C \eta^*) = \frac{M_{F_i}}{16\pi}(y_1^\dagger y_1)_{ii}\,, \tag{4.7}$$

$$\Gamma(F_i \to \nu_R \phi) = \Gamma(F_i^C \to \nu_R^C \phi) = \frac{M_{F_i}}{32\pi}(y_2^\dagger y_2)_{ii}\,, \tag{4.8}$$

in the limit of $M_{\eta,\phi} \ll M_{F_i}$. As shown in figure 5, the required lepton asymmetry in the left-handed sector arise at one-loop level and is calculated as [50]

$$
\begin{aligned}
\epsilon_{F_i} &= \frac{\Gamma(F_i \to L_L \eta) - \Gamma(F_i^C \to L_L^C \eta^*)}{\Gamma_{F_i}} \\
&= \frac{1}{8\pi} \frac{1}{(y_1^\dagger y_1)_{ii} + \frac{1}{2}(y_2^\dagger y_2)_{ii}} \sum_{j \neq i} \mathrm{Im}\left[(y_1^\dagger y_1)_{ij}(y_2^\dagger y_2)_{ji}\right] \frac{M_{F_i} M_{F_j}}{M_{F_i}^2 - M_{F_j}^2}\,,
\end{aligned} \tag{4.9}
$$

where the total decay width is $\Gamma_{F_i} = \left[(y_1^\dagger y_1)_{ii} + (y_2^\dagger y_2)_{ii}/2\right] M_{F_i}/(16\pi)$. Provided that $M_{F_1} \ll M_{F_{2,3}}$, then the final left-handed sector lepton asymmetry is dominantly determined by the decays of F_1:
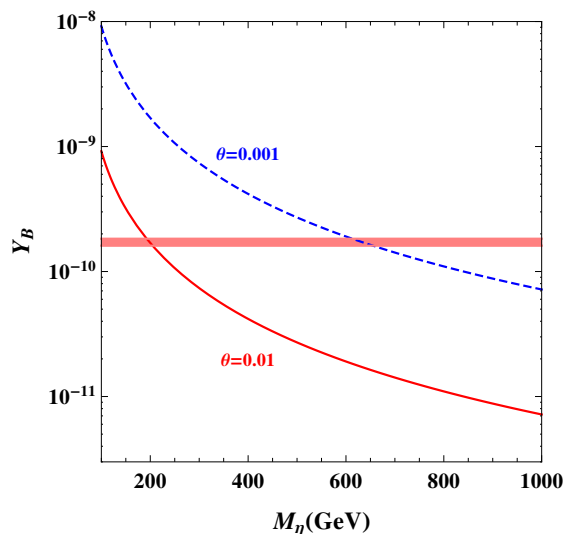
$$\epsilon_{F_1} \approx -\frac{1}{8\pi} \frac{1}{(y_1^\dagger y_1)_{11} + \frac{1}{2}(y_2^\dagger y_2)_{11}} \sum_{j \neq 1} \frac{M_{F_1}}{M_{F_j}} \mathrm{Im}\left[(y_1^\dagger y_1)_{1j}(y_2^\dagger y_2)_{j1}\right]. \tag{4.10}$$

We further take $y_1 = y_2$ for illustration, then the lepton asymmetry ϵ_{F_1} can be simplified as

$$\epsilon_{F_1} \simeq -\frac{1}{24\pi} \frac{1}{(y_1^\dagger y_1)_{11}} \sum_{j \neq 1} \frac{M_{F_1}}{M_{F_j}} \mathrm{Im}\left[(y_1^\dagger y_1)_{1j}^2\right]. \tag{4.11}$$

With the assumption $y_1 = y_2$, an upper bound on ϵ_L can be deduced after considering the radiative neutrino masses in eq. (2.11) [50]

$$|\epsilon_{F_1}| \lesssim \frac{4\pi M_{F_1} m_3 |\sin\delta|}{3\sin 2\theta \left| M_\eta^2 \ln \frac{M_\eta^2}{M_{F_1}^2} - M_\phi^2 \ln \frac{M_\phi^2}{M_{F_1}^2} \right|}\,, \tag{4.12}$$

Figure 6. Y_B as a function of M_η for $\theta = 0.01, 0.001$. The pink band corresponds to 1σ range of the observed value in ref. [143].

with m_3 the heaviest neutrino mass and δ the Dirac phase. Setting $M_{F_1} = 10^7 \, \text{GeV}$, $M_\phi = 60 \, \text{GeV}$, $m_3 = 0.1 \, \text{eV}$, $M_\eta = 200 \, \text{GeV}$, $\theta = 0.01$ and $\sin\delta = -1$, we obtain $\epsilon_{F_1} \simeq -2.7 \times 10^{-7}$. Then after the sphaleron processes, the desired baryon asymmetry

$$Y_B = \frac{n_B - n_{\bar{B}}}{s} = -\frac{28}{79}\frac{n_L}{s} \simeq -\frac{28}{79}\epsilon_{F_1}\left.\frac{n_{F_1}^{\text{eq}}}{s}\right|_{T=M_{F_1}} \simeq -\frac{\epsilon_{F_1}}{15 g_*} \approx 1.7 \times 10^{-10} \tag{4.13}$$

with $g_* = 106.75$ is obtained to explain the observed baryon asymmetry [143]. In figure 6, we show the value of Y_B as a function of M_η for $\theta = 0.01, 0.001$. With other parameters fixed, the larger M_η is, the smaller the θ is required to obtain the observed value of Y_B. Meanwhile, the decays of F_1 should be out of equilibrium, which requires that

$$\Gamma_{F_1} \lesssim H(T)\big|_{T=M_{F_1}}, \quad \text{with} \quad H(T) = \left(\frac{8\pi^2 g_*}{90}\right)^{\frac{1}{2}}\frac{T^2}{M_{\text{Pl}}}, \tag{4.14}$$

where $M_{\text{Pl}} = 1.22 \times 10^{19} \, \text{GeV}$. With the assumption $y_1 = y_2$, $M_{F_1} \sim 10^7 \, \text{GeV}$ and eq. (4.7), (4.8), the above condition indicates that the Yukawa coupling y_1 should satisfy

$$(y_1^\dagger y_1)_{11} \lesssim \left(\frac{2^{10}\pi^5 g_*}{5 * 3^4}\right)^{\frac{1}{2}}\frac{M_{F_1}}{M_{\text{Pl}}} \sim 10^{-10}. \tag{4.15}$$

4.3 Dark matter

In the two benchmark model we studied, there is no DM candidate in the tree level model (B). Meanwhile, for the one-loop model (a), there are viable DM candidate ϕ or $\eta_{R,I}^0$. In this work, we consider the case of $M_\phi < M_\eta$ with small mixing angle $\theta \lesssim 0.01$, thus the DM candidate is dominantly determined by ϕ. The relic density of ϕ is mostly determined by the quartic coupling $\lambda_\phi \phi^2 H^\dagger H$, and the analytic expression is given by [144]

$$\Omega_\phi h^2 = \frac{1.07 \times 10^9 \, \text{GeV}^{-1}}{\sqrt{g_*} M_{\text{Pl}} J(x_f)}, \tag{4.16}$$

where the function $J(x_f)$ is

$$J(x_f) = \int_{x_f}^{\infty} \frac{\langle \sigma v_{\text{rel}} \rangle (x)}{x^2} dx \,. \tag{4.17}$$

And the freeze-out parameter $x_f = M_\phi / T_f$ is acquired by numerically solving

$$x_f = \ln \left(\frac{0.038 M_{\text{Pl}} M_\phi \langle \sigma v_{\text{rel}} \rangle (x_f)}{\sqrt{g_* x_f}} \right) \,. \tag{4.18}$$

As pointed out by ref. [145], the QCD corrections for quarks in the final state, as well as three- and four-body final states from virtual gauge boson decays are important for total DM annihilation cross section. Following ref. [85, 86], we rewrite the annihilation cross section into all SM particles except h as

$$\sigma v_{\text{rel}} = \frac{8\lambda_\phi^2 v^2}{\sqrt{s}} \frac{\Gamma_h(\sqrt{s})}{(s - M_h^2)^2 + M_h^2 \Gamma_h^2(M_h)} \,, \tag{4.19}$$

where $v = 246\,\text{GeV}$ and the tabulated accurate Higgs boson width as a function of invariant mass $\Gamma_h(\sqrt{s})$ can be found in ref. [146]. For light DM $M_\phi < M_h/2$, the decay width $\Gamma_h(M_h)$ in the denominator should add the contribution of Higgs invisible decay $h \to \phi\phi$. Meanwhile, for heavy DM $M_\phi > M_h$, the extra contribution from $\phi\phi \to hh$ has also to be supplemented. But above $M_\phi > 150\,\text{GeV}$, we should use the tree-level expressions in appendix B, since the loop corrections are overestimated [85, 86]. The thermal average cross section is then carried out via

$$\langle \sigma v_{\text{rel}} \rangle (x) = \frac{x}{16 M_\phi^5 K_2^2(x)} \int_{4M_\phi^2}^{\infty} \sqrt{s - 4M_\phi^2} s K_1 \left(\frac{x\sqrt{s}}{M_\phi} \right) \sigma v_{\text{rel}} ds \,, \tag{4.20}$$

where $K_{1,2}(x)$ are modified Bessel functions of the second kind. In figure 7, we show the relic density $\Omega_\phi h^2$ as a function of M_ϕ for $\lambda_\phi = 0.001$, 0.01, and 0.1. The correct relic density can be obtained in the low-mass region $M_\phi < M_h/2$ and high-mass region $M_\phi > M_h/2$ for fixed value of λ_ϕ.

Then we consider possible constraints from DM direct detection. The cross section for spin independent DM-nucleon is

$$\sigma_{\text{SI}} = \frac{\lambda_\phi^2 f_N^2 \mu^2 m_N^2}{\pi M_h^4 M_\phi^2} \,, \tag{4.21}$$

where $m_N = (m_p + m_n)/2 = 939\,\text{MeV}$ is the averaged nucleon mass, $f_N = 0.3$ is the matrix element, and $\mu = m_N M_\phi / (m_N + M_\phi)$ is the DM-nucleon reduced mass. Provided ϕ accounting for 100% of DM, the predicted value of σ_{SI} is presented in figure 8. In the current simple scenario we considered, it is clear that the only possible region to escape tight direct detection constraints is around the Higgs mass resonance, i.e., $M_\phi \approx M_h/2$. Thus, the choice of $M_\phi = 60\,\text{GeV}$ in this work is safe to avoid direct detection constraints.

There are also possible constraints from indirect detection. In figure 9, we depict the predictions for $\langle \sigma v_{\text{rel}} \rangle_{\gamma\gamma, b\bar{b}}$, as well as the observed limits from Fermi-LAT [149, 150] and
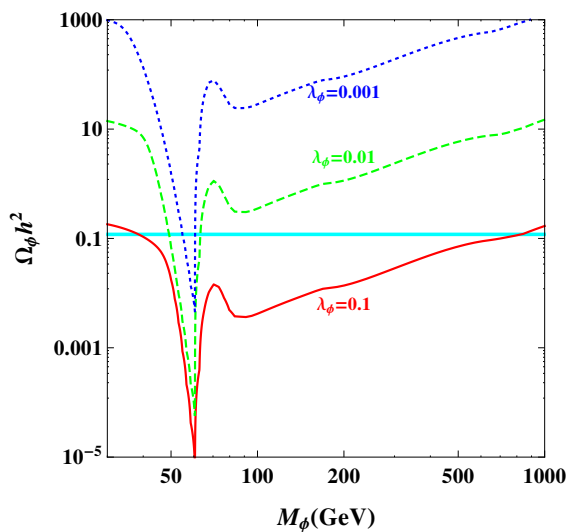
Figure 7. Relic density $\Omega_\phi h^2$ as a function of M_ϕ for $\lambda_\phi = 0.001$, 0.01, and 0.1. The cyan band corresponds to the observed DM relic density [143].
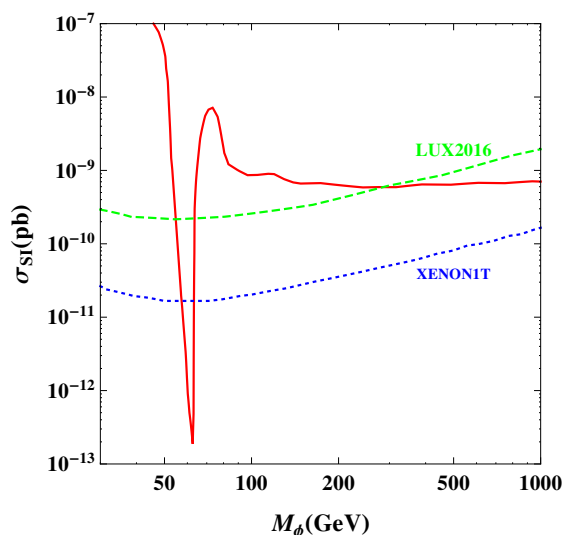

Figure 8. The spin-independent DM-nucleon cross section $\sigma_{\rm SI}$ as a function of M_ϕ. The green and blue lines correspond to LUX2016 [81–83] and XENON1T [147, 148] limits.

H.E.S.S. [151]. In the $\gamma\gamma$ final state, only a tiny mass region $M_h/2 \lesssim M_\phi$ is excluded. Meanwhile, in the $b\bar{b}$ final state, two mass region $M_\phi < 51\,{\rm GeV}$ and $M_h/2 \lesssim M_\phi < 70\,{\rm GeV}$ are excluded.

Last but not least, the SM Higgs h will decay into DM pair in the low mass region $M_\phi < M_h/2$, which will induce Higgs invisible decay at colliders. The corresponding decay width is

$$\Gamma(h \to \phi\phi) = \frac{\lambda_\phi^2 v^2}{8\pi M_h^2} \sqrt{M_h^2 - 4M_\phi^2}, \tag{4.22}$$
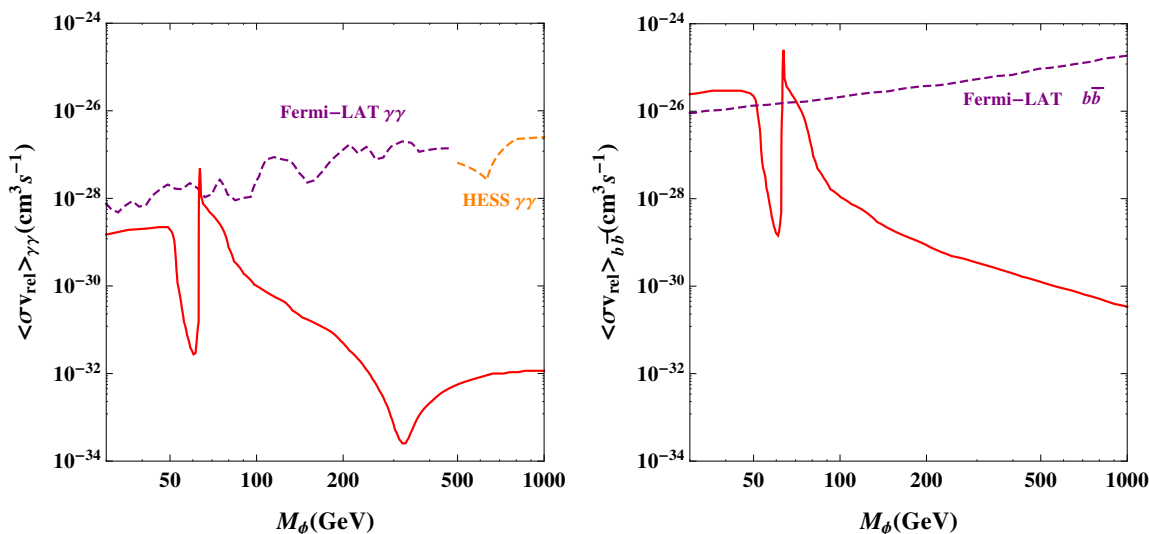
Figure 9. The velocity-averaged annihilation cross section times relative velocity $\langle \sigma v_{\rm rel} \rangle$ into $\gamma\gamma$ (left) and $b\bar{b}$ (right).
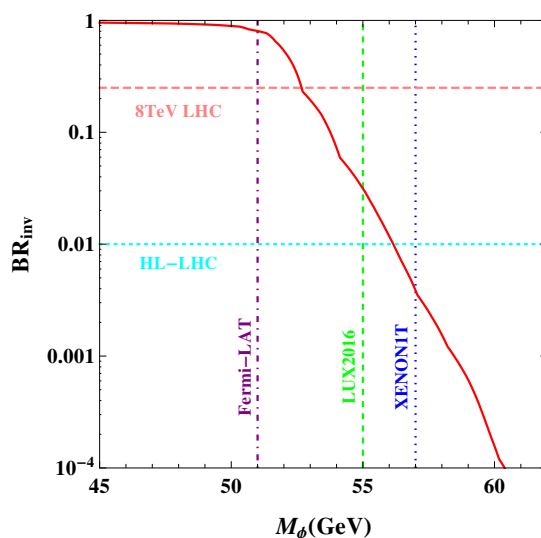
Figure 10. Branching ratio of Higgs invisible decay $\rm BR_{inv}$ as a function of M_ϕ.

and the invisible branching ratio is $\rm BR_{inv} = \Gamma(h \rightarrow \phi\phi)/(\Gamma(h \rightarrow \phi\phi) + \Gamma_{SM})$, where $\Gamma_{\rm SM} = 4.07\,{\rm MeV}$ for $M_h = 125\,{\rm GeV}$ [146]. In figure 10, we show $\rm BR_{inv}$ as a function of M_ϕ in the low mass region. The 8 TeV LHC limit, i.e., $\rm BR_{inv} \lesssim 0.25$, comes from the fitting results of Higgs visible decay [152]. And according to ref. [153], the HL-LHC might probe $\rm BR_{inv} \sim 0.02$ in the weak boson fusion channel. The 8 TeV LHC has excluded $M_\phi \lesssim 53\,{\rm GeV}$, which is less stringent than the LUX2016 limit. Meanwhile, the HL-LHC will be capable of excluding $M_\phi < 56\,{\rm GeV}$, which will be less stringent than the XENON1T.

In summary, we show the allowed parameter space in the $\lambda_\phi - M_\phi$ plane in figure 11, with the constraints from relic density, direct detection, indirect detection and Higgs in-
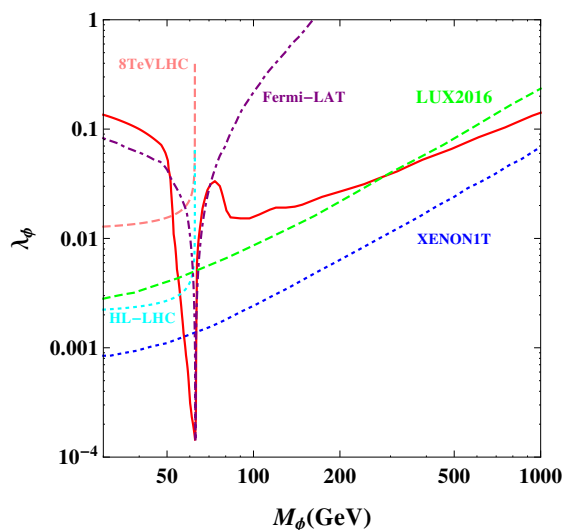
**Figure 11**. Allowed parameter space in the $\lambda_\phi - M_\phi$ plane.

visible decay. Apparently, the only allowed mass region is a narrow one being close to $M_\phi \lesssim M_h/2$.

4.4 LHC signature

Finally we briefly discuss possible LHC signatures. The newly introduced particles in $F, S_{1,2}$ can be pair/associated produced via Drell-Yan processes as long as they have non-zero gauge couplings. Then decays of new particles in $F, S_{1,2}$ will usually lead to multi-lepton signatures at LHC [154–159]. Since production cross section as well as the decay properties of new particles are model dependent, we take model (B) and model (a) for illustration here. Detailed study and simulation on specific models at LHC are highly encouraged to perform. First, for tree level model (B), a fermion doublet $F \equiv \Sigma = (\Sigma^0, \Sigma^-)^T \sim (1, 2, 1)$ and a scalar singlet $\phi \sim (1, 1, 0)$ are introduced. Hence, in model (B), only the fermion doublet Σ can be largely produced at LHC via Drell-Yan processes

$$pp \to \Sigma^+\Sigma^-, \ \Sigma^0\Sigma^0, \ \Sigma^\pm\Sigma^0. \tag{4.23}$$

The decay channels of the fermion doublet F are, $\Sigma^0 \to \ell^-W^+, \nu Z, \nu h$ and $\Sigma^- \to \ell^- Z$, $\ell^- h, \nu W^-$. And if $M_\phi < M_\Sigma$, new decay channels as $\Sigma^0 \to \nu\phi$ and $\Sigma^- \to \ell^-\phi$ with $\phi \to W^+W^-, ZZ, hh$ are also possible. Note that in Dirac neutrino mass models, there is no lepton number violation decays of Σ^0. Thus with $W^\pm, Z$ decaying leptoniclly, multilepton signatures can be generated. For $M_\Sigma < M_\phi$, ATLAS has performed an analysis on the signatures with three or more leptons based on $\Sigma^\pm \to \ell^\pm Z \to \ell^\pm\ell^+\ell^-$, and M_Σ in the range 114–176 GeV has been excluded [160]. The cross section of the inclusive trilepton signature $2\ell^\pm\ell^\mp + X$ is shown in left panel of figure 12. For $M_\Sigma > M_\phi$, the new decay channel $\Sigma^\pm \to \ell^\pm\phi \to \ell^\pm ZZ \to 3\ell^\pm 2\ell^\mp$ will lead to signatures with five or more leptons. And the cross section of this inclusive five-lepton signature is shown in right panel of figure 12.
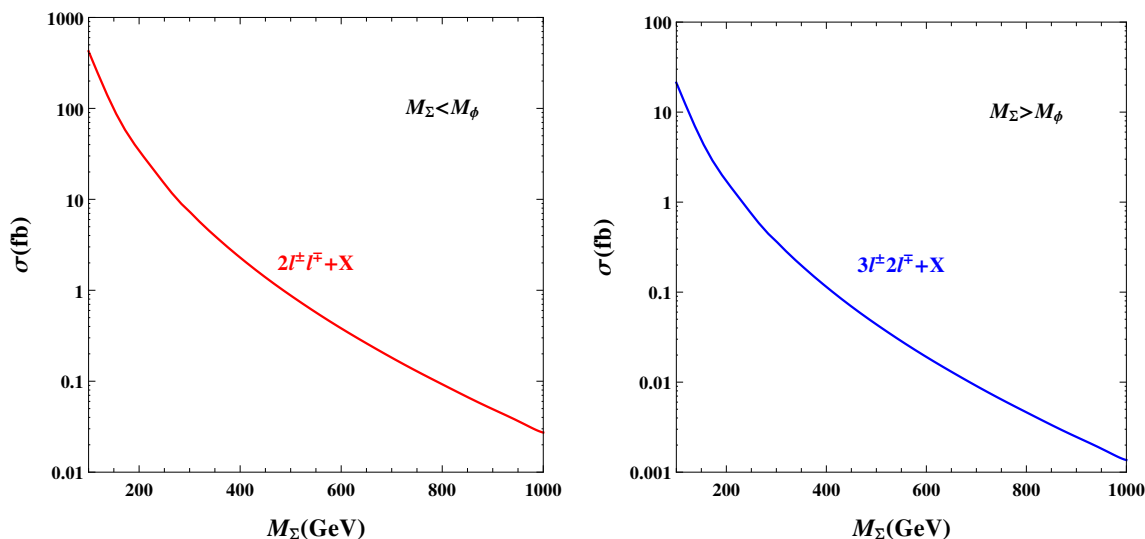
Figure 12. Cross section of trilepton signature $2\ell^{\pm}\ell^{\mp} + X$ (left) and five-lepton signature $3\ell^{\pm} + 2\ell^{\mp} + X$ (right) at 14 TeV LHC.

As for model (a), since both $F \sim (1,1,0)$ and $\phi \sim (1,1,0)$ are pure singlet, only the inert doublet $\eta = \left(\eta^{+}, (\eta_R^0 + \eta_I^0)/\sqrt{2}\right)^T \sim (1,2,1)$ can be pair produced at LHC

$$pp \to \eta^{+}\eta^{-}, \ \eta_R^0\eta_I^0, \ \eta^{\pm}\eta_{R,I}^0. \tag{4.24}$$

Because there are always a pair of DM in the final states, the signatures will thus contains missing transverse energy $\not{E}_T$. Here, we consider multi-lepton plus $\not{E}_T$ signatures. For inert doublet DM η_R^0/η_I^0, multi-lepton plus $\not{E}_T$ signatures at LHC have been extensively studied in ref. [94–98], thus we concentrate on F or ϕ DM. For fermion singlet DM, the promising signature is

$$pp \to \eta^{+}\eta^{-} \to \ell^{+}F + \ell^{-}F, \tag{4.25}$$

which leads to $\ell^{+}\ell^{-} + \not{E}_T$ signature at LHC. Cross section of this dilepton signature is presented in left panel of figure 13. Searches for such dilepton signature has been performed by ATLAS [161] and CMS [162]. Assuming $\eta^{\pm}$ exclusive decays into $e^{\pm}F$ or $\mu^{\pm}F$, ATLAS has excluded the region with $M_{\eta^{\pm}} \lesssim 300$ GeV and $M_F \lesssim 150$ GeV [161], meanwhile the CMS limit is less stringent [162]. On the other hand, for scalar singlet DM, the promising signature is

$$pp \to \eta^{\pm}\eta_{R,I}^0 \to W^{\pm}\phi + Z\phi \to 2\ell^{\pm}\ell^{\mp} + \not{E}_T. \tag{4.26}$$

Cross section of this dilepton signature is presented in right panel of figure 13. Searches for such trilepton signature has also been performed by ATLAS [163] and CMS [162]. The more stringent limit is also set by ATLAS, with $M_{\eta^{\pm}} \lesssim 350$ GeV and $M_{\phi} \lesssim 120$ GeV being excluded [163]. Note that this exclusion limit is acquired in simplified SUSY model with chargino-neutralino associated production. The exclusion limit is expected weaker in model (a), mainly because the cross section of $\eta^{\pm}\eta_{R,I}^0$ is much smaller than the cross section of chargino-neutralino with same masses.
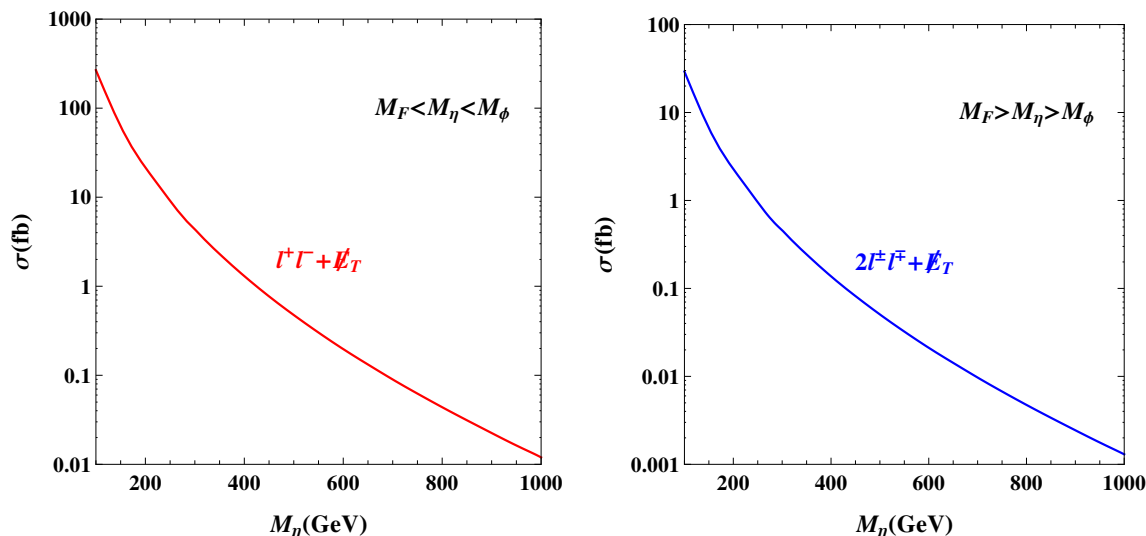
Figure 13. Cross section of dilepton signature $\ell^+\ell^- + \not{E}_T$ (left) and trilepton signature $2\ell^\pm\ell^\mp + \not{E}_T$ (right) at 14 TeV LHC.

Before ending this section, we give one benchmark point for each of the two benchmark models under the constraints from the phenomenologies we just discussed above. First, for the tree level benchmark model (B), the benchmark point is

$$y_1 = y_2 = 0.01, \qquad M_F = M_\phi = 1\,\text{TeV}, \qquad \langle\phi\rangle = 10\,\text{keV}. \qquad (4.27)$$

Then, for the one-loop level benchmark model (a), the benchmark point is

$$y_1^{i1} = y_2^{i1} = 10^{-6}, \qquad y_1^{i2,i3} = y_2^{i2,i3} = 10^{-2}, \qquad \theta = 0.01, \qquad (4.28)$$
$$M_\phi = 60\,\text{GeV}, \qquad M_\eta = 200\,\text{GeV}, \qquad M_F = 10^7\,\text{GeV}.$$

5 Conclusion

With at most two additional scalars and a heavy intermediate fermion, we perform a systematical study on pathways that can naturally generate tiny Dirac neutrino masses at tree- and one-loop level, In both cases, we concentrate on the $SU(2)_L$ scalar multiplet no larger than quintuplet, and derive the complete sets of viable models.

To realize tree level models in figure 1, the conservation of lepton number symmetry is assumed to forbid the unwanted Majorana mass term $(m_N/2)\overline{\nu_R^C}\nu_R$. Then an extra Z_2 symmetry is employed to forbid direct $\bar{\nu}_L\nu_R\overline{\phi^0}$ coupling. The breaking of this Z_2 symmetry will induce an effective small Dirac neutrino mass term $m_D\bar{\nu}_L\nu_R$. For tree level models, a finite set of model is found by requiring the natural small VEVs of new scalars. If one of the added scalars is actually the SM Higgs fields H itself, there are four types of realizations, which correspond to $d = 6$ effective low-energy operators. On the other hand, if two new scalars are introduced, then they are usually triplets/quadruplets/qintuplets for minimal models, corresponding to $d = 8$ or $d = 10$ effective low-energy operators.

To realize purely radiative models in figure 2, we further impose Z_2^D symmetry, under which $S_{1,2}$ and F carry Z_2^D-odd charge while all SM fields transform trivially. The lightest particle within the inert fields $S_{1,2}$ and F is stable, and thus becomes a dark matter candidate if it has no electric charge. We exhaust the list of viable models, and briefly discuss the possible DM candidate. Note that current direct detection limits have already excluded some models. Clearly, for fermion DM, it could be $F \sim (1, 1, 0), (1, 3, 0), (1, 5, 0)$, while for scalar DM, we have more option, e.g., the inert doublet $\eta \sim (1, 2, 1)$. The important fact is that if the DM candidate has non-zero hyper charge, a mixing between S_1 and S_2 and/or a quartic term as $(S_{1,2}H)^2$ is required to induce a large enough mass splitting between the real and imaginary part of the neutral component.

As for the phenomenological issues, the Yukawa coupling $y_1 \overline{F_R} L_L S_1$ will induce lepton flavor violation (LFV) processes. For tree level models, current limits on BR($\mu \rightarrow e\gamma$) denotes that $M_{S_1} \langle S_1 \rangle \gtrsim 600\,\text{GeV} \cdot \text{MeV}$, with $y_1 = y_2$ and $\langle S_1 \rangle = \langle S_2 \rangle$ being assumed. Meanwhile for radiative models, tight constraints from LFV requires the Yukawa coupling $|y_1| \lesssim 0.01$ when both F and S_1 are located around electroweak scale. On the other hand, if F is heavy enough, i.e., $M_F \sim 10^7\,\text{GeV}$, which is also possible in radiative models, the leptogenesis is also possible. For the scalar singlet DM ϕ in model (a), we perform a brief discussion on relic density, direct detection, indirect detection and Higgs invisible decay. And we find the the only allowed region is $M_\phi \lesssim M_h/2$. To illustrate LHC signatures, we take model (B) and model (a) as an example. For tree level model (B), the promising signatures is trilepton signature $\Sigma^\pm \rightarrow \ell^\pm Z \rightarrow \ell^\pm \ell^+ \ell^-$ when $M_\Sigma < M_\phi$. While for $M_\Sigma > M_\phi$, the five-lepton signature $\Sigma^\pm \rightarrow \ell^\pm \phi \rightarrow \ell^\pm ZZ \rightarrow 3\ell^\pm 2\ell^\mp$ might be promising. In case of loop level model (a), the promising signature is $\ell^+ \ell^- + \not{E}_T$ if F is DM, and $2\ell^\pm \ell^\mp + \not{E}_T$ if ϕ is DM.

Acknowledgments

A One-loop neutrino mass models with larger multiplets

Models	F	S_1	S_2	Z_2^D DM
(k)	$(1,3,0)$	$(1,4,1)$	$(1,3,0)$	Inert triplet or quadruplet
(l)	$(1,3,-2)$	$(1,4,-1)$	$(1,3,2)$	Inert triplet or quadruplet
(m)	$(1,3,2)$	$(1,4,3)$	$(1,3,-2)$	Excluded
(n)	$(1,3,-4)$	$(1,4,-3)$	$(1,3,4)$	Excluded
(o)	$(1,4,-1)$	$(1,4\pm1,0)$	$(1,4,1)$	Inert triplet/quintuplet or quadruplet
(p)	$(1,4,1)$	$(1,4\pm1,2)$	$(1,4,-1)$	Inert triplet/quintuplet or quadruplet
(q)	$(1,4,-3)$	$(1,4\pm1,-2)$	$(1,4,3)$	Excluded
(r)	$(1,4,3)$	$(1,4\pm1,4)$	$(1,4,-3)$	Excluded
(s)	$(1,4,-5)$	$(1,5,-4)$	$(1,4,5)$	Excluded
(t)	$(1,5,0)$	$(1,4,1)$	$(1,5,0)$	Inert quadruplet or quintuplet
(u)	$(1,5,-2)$	$(1,4,-1)$	$(1,5,2)$	Inert quadruplet or quintuplet
(v)	$(1,5,2)$	$(1,4,3)$	$(1,5,-2)$	Excluded
(w)	$(1,5,-4)$	$(1,4,-3)$	$(1,5,4)$	Excluded
(x)	$(1,5,4)$	$(1,4,5)$	$(1,5,-4)$	Excluded

Table 4. Radiative neutrino mass for Dirac neutrinos with quadruplet or/and quintuplet and DM candidate.

B Dark matter annihilation cross sections

Annihilation into SM fermions:

$$\sigma(\phi\phi \to f\bar{f})v_{\rm rel} = \frac{\lambda_\phi^2 M_f^2 N_c^f (1 - 4M_f^2/s)^{3/2}}{\pi[(s - M_h^2)^2 + M_h^2\Gamma_h^2]}, \tag{B.1}$$

where N_c^f is the color factor for fermion f.

Annihilation into W^+W^-:

$$\sigma(\phi\phi \to W^+W^-)v_{\rm rel} = \frac{\lambda_\phi^2(s^2 - 4M_W^2 s + 12M_W^4)\sqrt{1 - 4M_W^2/s}}{2\pi s[(s - M_h^2)^2 + M_h^2\Gamma_h^2]}. \tag{B.2}$$

Annihilation into ZZ:

$$\sigma(\phi\phi \to ZZ)v_{\rm rel} = \frac{\lambda_\phi^2(s^2 - 4M_Z^2 s + 12M_Z^4)\sqrt{1 - 4M_Z^2/s}}{4\pi s[(s - M_h^2)^2 + M_h^2\Gamma_h^2]}. \tag{B.3}$$

Annihilation into hh in the $s \to 4M_\phi^2$ limit:

$$\sigma(\phi\phi \to hh)v_{\rm rel} = \frac{\lambda_\phi^2[M_h^4 - 4M_\phi^2 + 2\lambda_\phi v^2(4M_\phi^2 - M_h^2)]^2}{4\pi M_\phi^2(M_h^4 - 6M_h^2 M_\phi^2 + 8M_\phi^2)^2}\sqrt{1 - \frac{M_h^2}{M_\phi^2}}. \tag{B.4}$$

Annihilation into $\gamma\gamma$:

$$\sigma(\phi\phi \to \gamma\gamma)v_{\rm rel} = \frac{16\lambda_\phi^2 v^2 \Gamma_{\gamma\gamma}(s)}{\sqrt{s}[(s - M_h^2)^2 + M_h^2\Gamma_h^2]} \,, \tag{B.5}$$

where the width $\Gamma_{\gamma\gamma}(s)$ is given by:

$$\Gamma_{\gamma\gamma}(s) = \frac{\alpha^2 s^{3/2}}{512\pi^3 v^2}\left| \sum_f N_c^f Q_f^2 A_{1/2}(\tau_f) + A_1(\tau_W)\right|^2 , \tag{B.6}$$

with $\tau_i = s/(4M_i^2)$ and the form factor:

$$A_{1/2}(\tau) = 2[\tau + (\tau - 1)f(\tau)]\tau^{-2}, \tag{B.7}$$

$$A_1(\tau) = -[2\tau^2 + 3\tau 3(2\tau - 1)f(\tau)]\tau^{-2}, \tag{B.8}$$

where $f(\tau)$ is

$$f(\tau) = \begin{cases} \arcsin^2\sqrt{\tau} & \tau \le 1 \\ -\frac{1}{4}\Big[\log\frac{1+\sqrt{1-\tau^{-1}}}{1-\sqrt{1-\tau^{-1}}} - i\pi\Big]^2 & \tau > 1 \,. \end{cases} \tag{B.9}$$

Open Access. This article is distributed under the terms of the Creative Commons Attribution License ([CC-BY 4.0](#)), which permits any use, distribution and reproduction in any medium, provided the original author(s) and source are credited.

References

[1] S. Weinberg, *Baryon and lepton nonconserving processes*, *Phys. Rev. Lett.* **43** (1979) 1566 [INSPIRE].

[2] P. Minkowski, $\mu \to e\gamma$ *at a rate of one out of* 10^9 *muon decays?*, *Phys. Lett.* **B 67** (1977) 421 [INSPIRE].

[3] T. Yanagida, *Horizontal symmetry and masses of neutrinos*, in Proceedings of the *Workshop on the Baryon Number of the Universe and Unified Theories*, Tsukuba Japan, 13–14 Feb 1979, O. Sawada and A. Sugamoto eds., KEK-79-18-95 [INSPIRE].

[4] M. Gell-Mann, P. Ramond and R. Slansky, *Complex spinors and unified theories*, in Proceedings of the *Supergravity Workshop*, New York U.S.A., 27–28 Sep 1979, P. Van Nieuwenhuizen and D.Z. Freedman eds., North-Holland, Amsterdam Netherlands (1979) [arXiv:1306.4669] [INSPIRE].

[5] S.L. Glashow, *The future of elementary particle physics*, in *Cargèse Summer Institute: Quarks and Leptons*, Cargèse France, 9–29 Jul 1979, M. Lévy et al. eds., Plenum Press (1980) [INSPIRE].

[6] R.N. Mohapatra and G. Senjanović, *Neutrino mass and spontaneous parity violation*, *Phys. Rev. Lett.* **44** (1980) 912 [INSPIRE].

[7] J. Schechter and J.W.F. Valle, *Neutrino masses in* SU(2) × U(1) *theories*, *Phys. Rev.* **D 22** (1980) 2227 [INSPIRE].

[8] J. Schechter and J.W.F. Valle, *Neutrino decay and spontaneous violation of lepton number*, *Phys. Rev.* **D 25** (1982) 774 [INSPIRE].

[9] R. Foot, H. Lew, X.G. He and G.C. Joshi, *Seesaw neutrino masses induced by a triplet of leptons*, *Z. Phys.* **C 44** (1989) 441 [INSPIRE].

[10] K.S. Babu, S. Nandi and Z. Tavartkiladze, *New mechanism for neutrino mass generation and triply charged Higgs bosons at the LHC*, *Phys. Rev.* **D 80** (2009) 071702 [arXiv:0905.2710] [INSPIRE].

[11] I. Picek and B. Radovčić, *Novel TeV-scale seesaw mechanism with Dirac mediators*, *Phys. Lett.* **B 687** (2010) 338 [arXiv:0911.1374] [INSPIRE].

[12] Y. Liao, *Unique neutrino mass operator at any mass dimension*, *Phys. Lett.* **B 694** (2011) 346 [arXiv:1009.1692] [INSPIRE].

[13] Y. Liao, *Cascade seesaw for tiny neutrino mass*, *JHEP* **06** (2011) 098 [arXiv:1011.3633] [INSPIRE].

[14] B. Ren, K. Tsumura and X.-G. He, *A Higgs quadruplet for type III seesaw and implications for $\mu \to e\gamma$ and μ–e conversion*, *Phys. Rev.* **D 84** (2011) 073004 [arXiv:1107.5879] [INSPIRE].

[15] K. Kumerički, I. Picek and B. Radovčić, *Exotic seesaw-motivated heavy leptons at the LHC*, *Phys. Rev.* **D 84** (2011) 093002 [arXiv:1106.1069] [INSPIRE].

[16] K. Kumerički, I. Picek and B. Radovčić, *TeV-scale seesaw with quintuplet fermions*, *Phys. Rev.* **D 86** (2012) 013006 [arXiv:1204.6599] [INSPIRE].

[17] I. Picek and B. Radovčić, *Enhancement of $h \to \gamma\gamma$ by seesaw-motivated exotic scalars*, *Phys. Lett.* **B 719** (2013) 404 [arXiv:1210.6449] [INSPIRE].

[18] K.L. McDonald, *Minimal tree-level seesaws with a heavy intermediate fermion*, *JHEP* **07** (2013) 020 [arXiv:1303.4573] [INSPIRE].

[19] S.S.C. Law and K.L. McDonald, *Generalized inverse seesaw mechanisms*, *Phys. Rev.* **D 87** (2013) 113003 [arXiv:1303.4887] [INSPIRE].

[20] A. Zee, *A theory of lepton number violation and neutrino Majorana masses*, *Phys. Lett.* **B 93** (1980) 389 [*Erratum ibid.* **B 95** (1980) 461] [INSPIRE].

[21] A. Pilaftsis, *Radiatively induced neutrino masses and large Higgs neutrino couplings in the standard model with Majorana fields*, *Z. Phys.* **C 55** (1992) 275 [hep-ph/9901206] [INSPIRE].

[22] E. Ma, *Verifiable radiative seesaw mechanism of neutrino mass and dark matter*, *Phys. Rev.* **D 73** (2006) 077301 [hep-ph/0601225] [INSPIRE].

[23] A. Zee, *Quantum numbers of Majorana neutrino masses*, *Nucl. Phys.* **B 264** (1986) 99 [INSPIRE].

[24] K.S. Babu, *Model of 'calculable' Majorana neutrino masses*, *Phys. Lett.* **B 203** (1988) 132 [INSPIRE].

[25] L.M. Krauss, S. Nasri and M. Trodden, *A model for neutrino masses and dark matter*, *Phys. Rev.* **D 67** (2003) 085002 [hep-ph/0210389] [INSPIRE].

[26] M. Gustafsson, J.M. No and M.A. Rivera, *Predictive model for radiatively induced neutrino masses and mixings with dark matter*, *Phys. Rev. Lett.* **110** (2013) 211802 [arXiv:1212.4806] [INSPIRE].

[27] Z.-L. Han, R. Ding and Y. Liao, *LHC phenomenology of the type II seesaw mechanism: nondegenerate case*, *Phys. Rev.* **D 91** (2015) 093006 [arXiv:1502.05242] [INSPIRE].

[28] Z.-L. Han, R. Ding and Y. Liao, *LHC phenomenology of the type II seesaw mechanism: observability of neutral scalars in the nondegenerate case*, *Phys. Rev.* **D 92** (2015) 033014 [arXiv:1506.08996] [INSPIRE].

[29] W. Wang and Z.-L. Han, *Radiative linear seesaw model, dark matter and* U(1)$_{B-L}$, *Phys. Rev.* **D 92** (2015) 095001 [arXiv:1508.00706] [INSPIRE].

[30] R. Ding, Z.-L. Han, Y. Liao and X.-D. Ma, *Interpretation of 750 GeV diphoton excess at LHC in singlet extension of color-octet neutrino mass model*, *Eur. Phys. J.* **C 76** (2016) 204 [arXiv:1601.02714] [INSPIRE].

[31] R. Ding, Z.-L. Han, Y. Liao and W.-P. Xie, *Radiative neutrino mass with* $\mathbb{Z}_3$ *dark matter: from relic density to LHC signatures*, *JHEP* **05** (2016) 030 [arXiv:1601.06355] [INSPIRE].

[32] S.-Y. Guo, Z.-L. Han and Y. Liao, *Testing the type II radiative seesaw model: from dark matter detection to LHC signatures*, *Phys. Rev.* **D 94** (2016) 115014 [arXiv:1609.01018] [INSPIRE].

[33] C. Guo, S.-Y. Guo, Z.-L. Han, B. Li and Y. Liao, *Hunting for heavy Majorana neutrinos with lepton number violating signatures at LHC*, arXiv:1701.02463 [INSPIRE].

[34] S.S.C. Law and K.L. McDonald, *A class of inert N-tuplet models with radiative neutrino mass and dark matter*, *JHEP* **09** (2013) 092 [arXiv:1305.6467] [INSPIRE].

[35] M. Roncadelli and D. Wyler, *Naturally light Dirac neutrinos in gauge theories*, *Phys. Lett.* **B 133** (1983) 325 [INSPIRE].

[36] P. Roy and O.U. Shanker, *Observable neutrino Dirac mass and supergrand unification*, *Phys. Rev. Lett.* **52** (1984) 713 [*Erratum ibid.* **52** (1984) 2190] [INSPIRE].

[37] D. Chang and R.N. Mohapatra, *Small and calculable Dirac neutrino mass*, *Phys. Rev. Lett.* **58** (1987) 1600 [INSPIRE].

[38] R.N. Mohapatra, *A model for Dirac neutrino masses and mixings*, *Phys. Lett.* **B 198** (1987) 69 [INSPIRE].

[39] R.N. Mohapatra, *Left-right symmetry and finite one loop Dirac neutrino mass*, *Phys. Lett.* **B 201** (1988) 517 [INSPIRE].

[40] B.S. Balakrishna and R.N. Mohapatra, *Radiative fermion masses from new physics at TeV scale*, *Phys. Lett.* **B 216** (1989) 349 [INSPIRE].

[41] E. Ma, *Radiative quark and lepton masses in a left-right gauge model*, *Phys. Rev. Lett.* **63** (1989) 1042 [INSPIRE].

[42] K.S. Babu and X.G. He, *Dirac neutrino masses as two loop radiative corrections*, *Mod. Phys. Lett.* **A 4** (1989) 61 [INSPIRE].

[43] P.-H. Gu and H.-J. He, *Neutrino mass and baryon asymmetry from Dirac seesaw*, *JCAP* **12** (2006) 010 [hep-ph/0610275] [INSPIRE].

[44] E. Ma and R. Srivastava, *Dirac or inverse seesaw neutrino masses with* $B-L$ *gauge symmetry and* S_3 *flavor symmetry*, *Phys. Lett.* **B 741** (2015) 217 [arXiv:1411.5042] [INSPIRE].

[45] E. Ma and R. Srivastava, *Dirac or inverse seesaw neutrino masses from gauged* $B-L$ *symmetry*, *Mod. Phys. Lett.* **A 30** (2015) 1530020 [arXiv:1504.00111] [INSPIRE].

[46] J.W.F. Valle and C.A. Vaquera-Araujo, *Dynamical seesaw mechanism for Dirac neutrinos*, *Phys. Lett.* **B 755** (2016) 363 [arXiv:1601.05237] [INSPIRE].

[47] C. Bonilla and J.W.F. Valle, *Naturally light neutrinos in Diracon model*, *Phys. Lett.* **B 762** (2016) 162 [arXiv:1605.08362] [INSPIRE].

[48] S. Centelles Chuliá, E. Ma, R. Srivastava and J.W.F. Valle, *Dirac neutrinos and dark matter stability from lepton quarticity*, *Phys. Lett.* **B 767** (2017) 209 [arXiv:1606.04543] [INSPIRE].

[49] M. Reig, J.W.F. Valle and C.A. Vaquera-Araujo, *Realistic* $SU(3)_c \otimes SU(3)_L \otimes U(1)_X$ *model with a type II Dirac neutrino seesaw mechanism*, *Phys. Rev.* **D 94** (2016) 033012 [arXiv:1606.08499] [INSPIRE].

[50] P.-H. Gu and U. Sarkar, *Radiative neutrino mass, dark matter and leptogenesis*, *Phys. Rev.* **D 77** (2008) 105031 [arXiv:0712.2933] [INSPIRE].

[51] Y. Farzan and E. Ma, *Dirac neutrino mass generation from dark matter*, *Phys. Rev.* **D 86** (2012) 033007 [arXiv:1204.4890] [INSPIRE].

[52] P.S. Bhupal Dev and A. Pilaftsis, *Minimal radiative neutrino mass mechanism for inverse seesaw models*, *Phys. Rev.* **D 86** (2012) 113001 [arXiv:1209.4051] [INSPIRE].

[53] H. Okada, *Two loop induced Dirac neutrino model and dark matters with global* $U(1)'$ *symmetry*, arXiv:1404.0280 [INSPIRE].

[54] S. Kanemura, K. Sakurai and H. Sugiyama, *Probing models of Dirac neutrino masses via the flavor structure of the mass matrix*, *Phys. Lett.* **B 758** (2016) 465 [arXiv:1603.08679] [INSPIRE].

[55] C. Bonilla, E. Ma, E. Peinado and J.W.F. Valle, *Two-loop Dirac neutrino mass and WIMP dark matter*, *Phys. Lett.* **B 762** (2016) 214 [arXiv:1607.03931] [INSPIRE].

[56] D. Borah and A. Dasgupta, *Common origin of neutrino mass, dark matter and Dirac leptogenesis*, *JCAP* **12** (2016) 034 [arXiv:1608.03872] [INSPIRE].

[57] E. Ma and O. Popov, *Pathways to naturally small Dirac neutrino masses*, *Phys. Lett.* **B 764** (2017) 142 [arXiv:1609.02538] [INSPIRE].

[58] E. Ma, N. Pollard, R. Srivastava and M. Zakeri, *Gauge* $B - L$ *model with residual* Z_3 *symmetry*, *Phys. Lett.* **B 750** (2015) 135 [arXiv:1507.03943] [INSPIRE].

[59] D. Borah and A. Dasgupta, *Naturally light Dirac neutrino in left-right symmetric model*, arXiv:1702.02877 [INSPIRE].

[60] J. Heeck and W. Rodejohann, *Neutrinoless quadruple beta decay*, *Europhys. Lett.* **103** (2013) 32001 [arXiv:1306.0580] [INSPIRE].

[61] J. Heeck, *Leptogenesis with lepton-number-violating Dirac neutrinos*, *Phys. Rev.* **D 88** (2013) 076004 [arXiv:1307.2241] [INSPIRE].

[62] A. Aranda, C. Bonilla, S. Morisi, E. Peinado and J.W.F. Valle, *Dirac neutrinos from flavor symmetry*, *Phys. Rev.* **D 89** (2014) 033001 [arXiv:1307.3553] [INSPIRE].

[63] K. Hally, H.E. Logan and T. Pilkington, *Constraints on large scalar multiplets from perturbative unitarity*, *Phys. Rev.* **D 85** (2012) 095017 [arXiv:1202.5073] [INSPIRE].

[64] K. Earl, K. Hartling, H.E. Logan and T. Pilkington, *Constraining models with a large scalar multiplet*, *Phys. Rev.* **D 88** (2013) 015002 [arXiv:1303.1244] [INSPIRE].

[65] E. Ma, *Naturally small seesaw neutrino mass with no new physics beyond the TeV scale*, *Phys. Rev. Lett.* **86** (2001) 2502 [hep-ph/0011121] [INSPIRE].

[66] S.M. Davidson and H.E. Logan, *Dirac neutrinos from a second Higgs doublet*, *Phys. Rev.* **D 80** (2009) 095008 [arXiv:0906.3335] [INSPIRE].

[67] S.M. Davidson and H.E. Logan, *LHC phenomenology of a two-Higgs-doublet neutrino mass model*, *Phys. Rev.* **D 82** (2010) 115031 [arXiv:1009.4413] [INSPIRE].

[68] N. Haba and K. Tsumura, *ν-two Higgs doublet model and its collider phenomenology*, *JHEP* **06** (2011) 068 [arXiv:1105.1409] [INSPIRE].

[69] P.A.N. Machado, Y.F. Perez, O. Sumensari, Z. Tabrizi and R.Z. Funchal, *On the viability of minimal neutrinophilic two-Higgs-doublet models*, *JHEP* **12** (2015) 160 [arXiv:1507.07550] [INSPIRE].

[70] W. Wang and Z.-L. Han, *Global* U(1)$_L$ *breaking in neutrinophilic 2HDM: from LHC signatures to X-ray line*, *Phys. Rev.* **D 94** (2016) 053015 [arXiv:1605.00239] [INSPIRE].

[71] PARTICLE DATA GROUP collaboration, C. Patrignani et al., *Review of particle physics*, *Chin. Phys.* **C 40** (2016) 100001 [INSPIRE].

[72] T. Robens and T. Stefaniak, *Status of the Higgs singlet extension of the standard model after LHC run 1*, *Eur. Phys. J.* **C 75** (2015) 104 [arXiv:1501.02234] [INSPIRE].

[73] T. Robens and T. Stefaniak, *LHC benchmark scenarios for the real Higgs singlet extension of the standard model*, *Eur. Phys. J.* **C 76** (2016) 268 [arXiv:1601.07880] [INSPIRE].

[74] O. Fischer, *Clues on the Majorana scale from scalar resonances at the LHC*, *Mod. Phys. Lett.* **A 32** (2017) 1750035 [arXiv:1607.00282] [INSPIRE].

[75] S. Kanemura, T. Nabeshima and H. Sugiyama, *Neutrino masses from loop-induced Dirac Yukawa couplings*, *Phys. Lett.* **B 703** (2011) 66 [arXiv:1106.2480] [INSPIRE].

[76] J. Kubo, E. Ma and D. Suematsu, *Cold dark matter, radiative neutrino mass, $\mu \to e\gamma$ and neutrinoless double beta decay*, *Phys. Lett.* **B 642** (2006) 18 [hep-ph/0604114] [INSPIRE].

[77] A. Vicente and C.E. Yaguna, *Probing the scotogenic model with lepton flavor violating processes*, *JHEP* **02** (2015) 144 [arXiv:1412.2545] [INSPIRE].

[78] E. Ma and D. Suematsu, *Fermion triplet dark matter and radiative neutrino mass*, *Mod. Phys. Lett.* **A 24** (2009) 583 [arXiv:0809.0942] [INSPIRE].

[79] W. Chao, *Dark matter, LFV and neutrino magnetic moment in the radiative seesaw model with fermion triplet*, *Int. J. Mod. Phys.* **A 30** (2015) 1550007 [arXiv:1202.6394] [INSPIRE].

[80] F. von der Pahlen, G. Palacio, D. Restrepo and O. Zapata, *Radiative type III seesaw model and its collider phenomenology*, *Phys. Rev.* **D 94** (2016) 033005 [arXiv:1605.01129] [INSPIRE].

[81] LUX collaboration, D.S. Akerib et al., *First results from the LUX dark matter experiment at the Sanford Underground Research Facility*, *Phys. Rev. Lett.* **112** (2014) 091303 [arXiv:1310.8214] [INSPIRE].

[82] LUX collaboration, D.S. Akerib et al., *Improved limits on scattering of weakly interacting massive particles from reanalysis of 2013 LUX data*, *Phys. Rev. Lett.* **116** (2016) 161301 [arXiv:1512.03506] [INSPIRE].

[83] LUX collaboration, D.S. Akerib et al., *Results from a search for dark matter in the complete LUX exposure*, *Phys. Rev. Lett.* **118** (2017) 021303 [arXiv:1608.07648] [INSPIRE].

[84] PandaX-II collaboration, A. Tan et al., *Dark matter results from first 98.7 days of data from the PandaX-II experiment*, *Phys. Rev. Lett.* **117** (2016) 121303 [arXiv:1607.07400] [inSPIRE].

[85] J.M. Cline, K. Kainulainen, P. Scott and C. Weniger, *Update on scalar singlet dark matter*, *Phys. Rev.* **D 88** (2013) 055025 [*Erratum ibid.* **D 92** (2015) 039906] [arXiv:1306.4710] [inSPIRE].

[86] L. Feng, S. Profumo and L. Ubaldi, *Closing in on singlet scalar dark matter: LUX, invisible Higgs decays and gamma-ray lines*, *JHEP* **03** (2015) 045 [arXiv:1412.1105] [inSPIRE].

[87] A. Arhrib, Y.-L.S. Tsai, Q. Yuan and T.-C. Yuan, *An updated analysis of inert Higgs doublet model in light of the recent results from LUX, PLANCK, AMS-02 and LHC*, *JCAP* **06** (2014) 030 [arXiv:1310.0358] [inSPIRE].

[88] E.M. Dolle and S. Su, *The inert dark matter*, *Phys. Rev.* **D 80** (2009) 055012 [arXiv:0906.1609] [inSPIRE].

[89] L. Lopez Honorez, E. Nezri, J.F. Oliver and M.H.G. Tytgat, *The inert doublet model: an archetype for dark matter*, *JCAP* **02** (2007) 028 [hep-ph/0612275] [inSPIRE].

[90] T. Cohen, J. Kearney, A. Pierce and D. Tucker-Smith, *Singlet-doublet dark matter*, *Phys. Rev.* **D 85** (2012) 075003 [arXiv:1109.2604] [inSPIRE].

[91] M. Kakizaki, A. Santa and O. Seto, *Phenomenological signatures of mixed complex scalar WIMP dark matter*, *Int. J. Mod. Phys.* **A 32** (2017) 1750038 [arXiv:1609.06555] [inSPIRE].

[92] X.-G. He and J. Tandean, *New LUX and PandaX-II results illuminating the simplest Higgs-portal dark matter models*, *JHEP* **12** (2016) 074 [arXiv:1609.03551] [inSPIRE].

[93] J.A. Casas, D.G. Cerdeño, J.M. Moreno and J. Quilis, *Reopening the Higgs portal for singlet scalar dark matter*, arXiv:1701.08134 [inSPIRE].

[94] E. Dolle, X. Miao, S. Su and B. Thomas, *Dilepton signals in the inert doublet model*, *Phys. Rev.* **D 81** (2010) 035003 [arXiv:0909.3094] [inSPIRE].

[95] X. Miao, S. Su and B. Thomas, *Trilepton signals in the inert doublet model*, *Phys. Rev.* **D 82** (2010) 035009 [arXiv:1005.0090] [inSPIRE].

[96] M. Gustafsson, S. Rydbeck, L. Lopez-Honorez and E. Lundström, *Status of the inert doublet model and the role of multileptons at the LHC*, *Phys. Rev.* **D 86** (2012) 075019 [arXiv:1206.6316] [inSPIRE].

[97] G. Bélanger et al., *Dilepton constraints in the inert doublet model from run 1 of the LHC*, *Phys. Rev.* **D 91** (2015) 115011 [arXiv:1503.07367] [inSPIRE].

[98] A. Datta, N. Ganguly, N. Khan and S. Rakshit, *Exploring collider signatures of the inert Higgs doublet model*, *Phys. Rev.* **D 95** (2017) 015017 [arXiv:1610.00648] [inSPIRE].

[99] F.S. Queiroz and C.E. Yaguna, *The CTA aims at the inert doublet model*, *JCAP* **02** (2016) 038 [arXiv:1511.05967] [inSPIRE].

[100] C. Garcia-Cely, M. Gustafsson and A. Ibarra, *Probing the inert doublet dark matter model with Cherenkov telescopes*, *JCAP* **02** (2016) 043 [arXiv:1512.02801] [inSPIRE].

[101] M. Cirelli, N. Fornengo and A. Strumia, *Minimal dark matter*, *Nucl. Phys.* **B 753** (2006) 178 [hep-ph/0512090] [inSPIRE].

[102] T. Hambye, F.S. Ling, L. Lopez Honorez and J. Rocher, *Scalar multiplet dark matter*, *JHEP* **07** (2009) 090 [*Erratum ibid.* **05** (2010) 066] [`arXiv:0903.4010`] [ɪɴSPIRE].

[103] P. Fileviez Perez, H.H. Patel, M. Ramsey-Musolf and K. Wang, *Triplet scalars and dark matter at the LHC*, *Phys. Rev.* **D 79** (2009) 055024 [`arXiv:0811.3957`] [ɪɴSPIRE].

[104] T. Araki, C.Q. Geng and K.I. Nagao, *Dark matter in inert triplet models*, *Phys. Rev.* **D 83** (2011) 075014 [`arXiv:1102.4906`] [ɪɴSPIRE].

[105] W.-B. Lu and P.-H. Gu, *Leptogenesis, radiative neutrino masses and inert Higgs triplet dark matter*, *JCAP* **05** (2016) 040 [`arXiv:1603.05074`] [ɪɴSPIRE].

[106] W.-B. Lu and P.-H. Gu, *Mixed inert scalar triplet dark matter, radiative neutrino masses and leptogenesis*, `arXiv:1611.02106` [ɪɴSPIRE].

[107] Y. Kajiyama, H. Okada and K. Yagyu, *Two loop radiative seesaw model with inert triplet scalar field*, *Nucl. Phys.* **B 874** (2013) 198 [`arXiv:1303.3463`] [ɪɴSPIRE].

[108] L.M. Krauss and F. Wilczek, *Discrete gauge symmetry in continuum theories*, *Phys. Rev. Lett.* **62** (1989) 1221 [ɪɴSPIRE].

[109] B. Batell, *Dark discrete gauge symmetries*, *Phys. Rev.* **D 83** (2011) 035006 [`arXiv:1007.0045`] [ɪɴSPIRE].

[110] MEG collaboration, J. Adam et al., *New constraint on the existence of the $\mu^+ \to e^+\gamma$ decay*, *Phys. Rev. Lett.* **110** (2013) 201801 [`arXiv:1303.0754`] [ɪɴSPIRE].

[111] MEG collaboration, A.M. Baldini et al., *Search for the lepton flavour violating decay $\mu^+ \to e^+\gamma$ with the full dataset of the MEG experiment*, *Eur. Phys. J.* **C 76** (2016) 434 [`arXiv:1605.05081`] [ɪɴSPIRE].

[112] A.M. Baldini et al., *MEG upgrade proposal*, `arXiv:1301.7225` [ɪɴSPIRE].

[113] E. Ma and M. Raidal, *Neutrino mass, muon anomalous magnetic moment and lepton flavor nonconservation*, *Phys. Rev. Lett.* **87** (2001) 011802 [*Erratum ibid.* **87** (2001) 159901] [`hep-ph/0102255`] [ɪɴSPIRE].

[114] M. Raidal et al., *Flavour physics of leptons and dipole moments*, *Eur. Phys. J.* **C 57** (2008) 13 [`arXiv:0801.1826`] [ɪɴSPIRE].

[115] T. Fukuyama, H. Sugiyama and K. Tsumura, *Constraints from muon $g - 2$ and LFV processes in the Higgs triplet model*, *JHEP* **03** (2010) 044 [`arXiv:0909.4943`] [ɪɴSPIRE].

[116] Y. Liao, G.-Z. Ning and L. Ren, *Flavor violating transitions of charged leptons from a seesaw mechanism of dimension seven*, *Phys. Rev.* **D 82** (2010) 113003 [`arXiv:1008.0117`] [ɪɴSPIRE].

[117] A. Abada et al., *Lepton flavor violation in low-scale seesaw models: SUSY and non-SUSY contributions*, *JHEP* **11** (2014) 048 [`arXiv:1408.0138`] [ɪɴSPIRE].

[118] E. Bertuzzo, Y.F. Perez G., O. Sumensari and R. Zukanovich Funchal, *Limits on neutrinophilic two-Higgs-doublet models from flavor physics*, *JHEP* **01** (2016) 018 [`arXiv:1510.04284`] [ɪɴSPIRE].

[119] Y. Liao and J.-Y. Liu, *Radiative and flavor-violating transitions of leptons from interactions with color-octet particles*, *Phys. Rev.* **D 81** (2010) 013004 [`arXiv:0911.3711`] [ɪɴSPIRE].

[120] T. Toma and A. Vicente, *Lepton flavor violation in the scotogenic model*, *JHEP* **01** (2014) 160 [`arXiv:1312.2840`] [ɪɴSPIRE].

[121] T.A. Chowdhury and S. Nasri, *Lepton flavor violation in the inert scalar model with higher representations*, *JHEP* **12** (2015) 040 [arXiv:1506.00261] [INSPIRE].

[122] B. Li, Y. Liao and X.-D. Ma, *Charged lepton flavor-violating transitions in color octet model*, *Eur. Phys. J.* **C 76** (2016) 615 [arXiv:1608.07785] [INSPIRE].

[123] D. Aristizabal Sierra, J. Kubo, D. Restrepo, D. Suematsu and O. Zapata, *Radiative seesaw: warm dark matter, collider and lepton flavour violating signals*, *Phys. Rev.* **D 79** (2009) 013011 [arXiv:0808.3340] [INSPIRE].

[124] M. Lindner, M. Platscher and F.S. Queiroz, *A call for new physics: the muon anomalous magnetic moment and lepton flavor violation*, arXiv:1610.06587 [INSPIRE].

[125] R. Ding, Z.-L. Han, Y. Liao, H.-J. Liu and J.-Y. Liu, *Phenomenology in the minimal cascade seesaw mechanism for neutrino masses*, *Phys. Rev.* **D 89** (2014) 115024 [arXiv:1403.2040] [INSPIRE].

[126] Muon g-2 collaboration, G.W. Bennett et al., *Final report of the E821 muon anomalous magnetic moment measurement at BNL*, *Phys. Rev.* **D 73** (2006) 072003 [hep-ex/0602035] [INSPIRE].

[127] ACME collaboration, J. Baron et al., *Order of magnitude smaller limit on the electric dipole moment of the electron*, *Science* **343** (2014) 269 [arXiv:1310.7534] [INSPIRE].

[128] V.D. Barger, A.K. Das and C. Kao, *The electric dipole moment of the muon in a two-Higgs doublet model*, *Phys. Rev.* **D 55** (1997) 7099 [hep-ph/9611344] [INSPIRE].

[129] T. Fukuyama, *Searching for new physics beyond the standard model in electric dipole moment*, *Int. J. Mod. Phys.* **A 27** (2012) 1230015 [arXiv:1201.4252] [INSPIRE].

[130] M. Fukugita and T. Yanagida, *Baryogenesis without grand unification*, *Phys. Lett.* **B 174** (1986) 45 [INSPIRE].

[131] S. Davidson, E. Nardi and Y. Nir, *Leptogenesis*, *Phys. Rept.* **466** (2008) 105 [arXiv:0802.2962] [INSPIRE].

[132] K. Dick, M. Lindner, M. Ratz and D. Wright, *Leptogenesis with Dirac neutrinos*, *Phys. Rev. Lett.* **84** (2000) 4039 [hep-ph/9907562] [INSPIRE].

[133] H. Murayama and A. Pierce, *Realistic Dirac leptogenesis*, *Phys. Rev. Lett.* **89** (2002) 271601 [hep-ph/0206177] [INSPIRE].

[134] D.G. Cerdeño, A. Dedes and T.E.J. Underwood, *The minimal phantom sector of the standard model: Higgs phenomenology and Dirac leptogenesis*, *JHEP* **09** (2006) 067 [hep-ph/0607157] [INSPIRE].

[135] P.-H. Gu and H.-J. He, *Neutrino mass and baryon asymmetry from Dirac seesaw*, *JCAP* **12** (2006) 010 [hep-ph/0610275] [INSPIRE].

[136] P.-H. Gu, H.-J. He and U. Sarkar, *Dirac neutrinos, dark energy and baryon asymmetry*, *JCAP* **11** (2007) 016 [arXiv:0705.3736] [INSPIRE].

[137] P.-H. Gu, H.-J. He and U. Sarkar, *Realistic neutrinogenesis with radiative vertex correction*, *Phys. Lett.* **B 659** (2008) 634 [arXiv:0709.1019] [INSPIRE].

[138] A. Bechinger and G. Seidl, *Resonant Dirac leptogenesis on throats*, *Phys. Rev.* **D 81** (2010) 065015 [arXiv:0907.4341] [INSPIRE].

[139] P.-H. Gu, *From Dirac neutrino masses to baryonic and dark matter asymmetries*, *Nucl. Phys.* **B 872** (2013) 38 [arXiv:1209.4579] [INSPIRE].

[140] D. Borah and A. Dasgupta, *Common origin of neutrino mass, dark matter and Dirac leptogenesis*, *JCAP* **12** (2016) 034 [arXiv:1608.03872] [INSPIRE].

[141] A. Pilaftsis and T.E.J. Underwood, *Resonant leptogenesis*, *Nucl. Phys.* **B 692** (2004) 303 [hep-ph/0309342] [INSPIRE].

[142] A. Pilaftsis and T.E.J. Underwood, *Electroweak-scale resonant leptogenesis*, *Phys. Rev.* **D 72** (2005) 113001 [hep-ph/0506107] [INSPIRE].

[143] PLANCK collaboration, P.A.R. Ade et al., *Planck 2015 results. XIII. Cosmological parameters*, *Astron. Astrophys.* **594** (2016) A13 [arXiv:1502.01589] [INSPIRE].

[144] P. Gondolo and G. Gelmini, *Cosmic abundances of stable particles: improved analysis*, *Nucl. Phys.* **B 360** (1991) 145 [INSPIRE].

[145] J.M. Cline and K. Kainulainen, *Electroweak baryogenesis and dark matter from a singlet Higgs*, *JCAP* **01** (2013) 012 [arXiv:1210.4196] [INSPIRE].

[146] LHC HIGGS CROSS SECTION WORKING GROUP, J.R. Andersen et al., *Handbook of LHC Higgs cross sections: 3. Higgs properties*, arXiv:1307.1347 [INSPIRE].

[147] XENON1T collaboration, E. Aprile, *The XENON1T dark matter search experiment*, *Springer Proc. Phys.* **148** (2013) 93 [arXiv:1206.6288] [INSPIRE].

[148] XENON collaboration, E. Aprile et al., *Physics reach of the XENON1T dark matter experiment*, *JCAP* **04** (2016) 027 [arXiv:1512.07501] [INSPIRE].

[149] FERMI-LAT collaboration, M. Ackermann et al., *Searching for dark matter annihilation from Milky Way dwarf spheroidal galaxies with six years of Fermi Large Area Telescope data*, *Phys. Rev. Lett.* **115** (2015) 231301 [arXiv:1503.02641] [INSPIRE].

[150] FERMI-LAT collaboration, M. Ackermann et al., *Updated search for spectral lines from galactic dark matter interactions with pass 8 data from the Fermi Large Area Telescope*, *Phys. Rev.* **D 91** (2015) 122002 [arXiv:1506.00013] [INSPIRE].

[151] H.E.S.S. collaboration, A. Abramowski et al., *Search for photon-linelike signatures from dark matter annihilations with H.E.S.S.*, *Phys. Rev. Lett.* **110** (2013) 041301 [arXiv:1301.1173] [INSPIRE].

[152] ATLAS and CMS collaborations, *Measurements of the Higgs boson production and decay rates and constraints on its couplings from a combined ATLAS and CMS analysis of the LHC pp collision data at $\sqrt{s} = 7$ and 8 TeV*, *JHEP* **08** (2016) 045 [arXiv:1606.02266] [INSPIRE].

[153] C. Bernaciak, T. Plehn, P. Schichtel and J. Tattersall, *Spying an invisible Higgs boson*, *Phys. Rev.* **D 91** (2015) 035024 [arXiv:1411.7699] [INSPIRE].

[154] F. del Aguila and J.A. Aguilar-Saavedra, *Electroweak scale seesaw and heavy Dirac neutrino signals at LHC*, *Phys. Lett.* **B 672** (2009) 158 [arXiv:0809.2096] [INSPIRE].

[155] R. Franceschini, T. Hambye and A. Strumia, *Type-III seesaw mechanism at CERN LHC*, *Phys. Rev.* **D 78** (2008) 033002 [arXiv:0805.1613] [INSPIRE].

[156] P. Fileviez Pérez, T. Han, G.-y. Huang, T. Li and K. Wang, *Neutrino masses and the CERN LHC: testing the type II seesaw mechanism*, *Phys. Rev.* **D 78** (2008) 015018 [arXiv:0805.3536] [INSPIRE].

[157] C.-Y. Chen and P.S.B. Dev, *Multi-lepton collider signatures of heavy Dirac and Majorana neutrinos*, *Phys. Rev.* **D 85** (2012) 093018 [arXiv:1112.6419] [INSPIRE].

[158] K.L. McDonald, *Probing exotic fermions from a seesaw/radiative model at the LHC*, *JHEP* **11** (2013) 131 [arXiv:1310.0609] [ɪɴSPIRE].

[159] F.F. Deppisch, P.S. Bhupal Dev and A. Pilaftsis, *Neutrinos and collider physics*, *New J. Phys.* **17** (2015) 075019 [arXiv:1502.06541] [ɪɴSPIRE].

[160] ATLAS collaboration, *Search for heavy lepton resonances decaying to a Z boson and a lepton in pp collisions at $\sqrt{s} = 8\,TeV$ with the ATLAS detector*, *JHEP* **09** (2015) 108 [arXiv:1506.01291] [ɪɴSPIRE].

[161] ATLAS collaboration, *Search for direct production of charginos, neutralinos and sleptons in final states with two leptons and missing transverse momentum in pp collisions at $\sqrt{s} = 8\,TeV$ with the ATLAS detector*, *JHEP* **05** (2014) 071 [arXiv:1403.5294] [ɪɴSPIRE].

[162] CMS collaboration, *Searches for electroweak production of charginos, neutralinos and sleptons decaying to leptons and W, Z and Higgs bosons in pp collisions at 8 TeV*, *Eur. Phys. J.* **C 74** (2014) 3036 [arXiv:1405.7570] [ɪɴSPIRE].

[163] ATLAS collaboration, *Search for direct production of charginos and neutralinos in events with three leptons and missing transverse momentum in $\sqrt{s} = 8\,TeV$ pp collisions with the ATLAS detector*, *JHEP* **04** (2014) 169 [arXiv:1402.7029] [ɪɴSPIRE].